

Review

Do Iron Oxide Nanoparticles Have Significant Antibacterial Properties?

Sergey V. Gudkov ^{1,*}, Dmitriy E. Burmistrov ¹, Dmitriy A. Serov ¹, Maksim B. Rebezov ^{1,2},
Anastasia A. Semenova ² and Andrey B. Lisitsyn ²

¹ Prokhorov General Physics Institute of the Russian Academy of Sciences, 119991 Moscow, Russia; dmitriiburmistroff@gmail.com (D.E.B.); dmitriy_serov_91@mail.ru (D.A.S.); rebezov@yandex.ru (M.B.R.)

² V.M. Gorbатов Federal Research Center for Food Systems of the Russian Academy of Sciences, 109316 Moscow, Russia; a.semenova@fncps.ru (A.A.S.); info@fncps.ru (A.B.L.)

* Correspondence: s_makariy@rambler.ru; Tel.: +7-499-503-8734

Abstract: The use of metal oxide nanoparticles is one of the promising ways for overcoming antibiotic resistance in bacteria. Iron oxide nanoparticles (IONPs) have found wide applications in different fields of biomedicine. Several studies have suggested using the antimicrobial potential of IONPs. Iron is one of the key microelements and plays an important role in the function of living systems of different hierarchies. Iron abundance and its physiological functions bring into question the ability of iron compounds at the same concentrations, on the one hand, to inhibit the microbial growth and, on the other hand, to positively affect mammalian cells. At present, multiple studies have been published that show the antimicrobial effect of IONPs against Gram-negative and Gram-positive bacteria and fungi. Several studies have established that IONPs have a low toxicity to eukaryotic cells. It gives hope that IONPs can be considered potential antimicrobial agents of the new generation that combine antimicrobial action and high biocompatibility with the human body. This review is intended to inform readers about the available data on the antimicrobial properties of IONPs, a range of susceptible bacteria, mechanisms of the antibacterial action, dependence of the antibacterial action of IONPs on the method for synthesis, and the biocompatibility of IONPs with eukaryotic cells and tissues.

Keywords: nanoparticles; iron oxide; antimicrobial effect; green synthesis



Citation: Gudkov, S.V.; Burmistrov, D.E.; Serov, D.A.; Rebezov, M.B.; Semenova, A.A.; Lisitsyn, A.B. Do Iron Oxide Nanoparticles Have Significant Antibacterial Properties?. *Antibiotics* **2021**, *10*, 884. <https://doi.org/10.3390/antibiotics10070884>

Academic Editor: Hao Song

Received: 23 June 2021

Accepted: 18 July 2021

Published: 20 July 2021

Publisher's Note: MDPI stays neutral with regard to jurisdictional claims in published maps and institutional affiliations.



Copyright: © 2021 by the authors. Licensee MDPI, Basel, Switzerland. This article is an open access article distributed under the terms and conditions of the Creative Commons Attribution (CC BY) license (<https://creativecommons.org/licenses/by/4.0/>).

1. Introduction

Nowadays, the application of nanotechnological solutions, such as the use of nanoparticles, is one of the promising ways to overcome antibiotic resistance in bacteria [1–5].

Nanoparticles (NPs) of several metals and their oxides, such as Ag, ZnO, Fe₂O₃, Fe₃O₄, Al₂O₃, TiO₂, and CuO, exert antibacterial action against Gram-negative and Gram-positive bacteria, as well as the antifungal action [6–14].

Iron is one of the most abundant elements on Earth and the fourth-most abundant element in the Earth's crust. Iron makes up more than 85% of the mass of the Earth's core and about 5% of the mass of the Earth's crust [15,16]. In living systems, iron is one of the key microelements. It has several important functions: it is a cofactor of several enzymes (catalase) and transport proteins (hemoglobin), ETC proteins (cytochromes and FeS proteins), and is necessary for DNA repair [17–20]. Iron is also found in the regulatory proteins of enterobacteria *Salmonella enterica*, including Fur, Fnr, NorR, SoxR, IscR, and NsrR [21–26]. Several bacteria can accumulate iron oxides in special organelles called magnetosomes—for example, *Magnetospirillum magneticum* [27]. It is assumed that they provide bacteria with the constant magnetic dipole, presumably for navigation purposes [28]. It was shown in *Magnetospirillum magneticum* wild-type and DmagA1-/- that magnetosomes plays a key role in magneto-aerotaxis. Magneto-aerotaxis is the direct motion of bacteria downward in microaerobic environments favorable to growth [29].

Bacteria that use the iron oxidation reaction $\text{Fe}^{2+} + 0.25 \text{O}_2 + \text{H}^+ \rightarrow \text{Fe}^{3+} + 0.5 \text{H}_2\text{O}$ for energy generation and metabolism maintenance have been described. A minimum two groups of obligate iron-oxidizing bacteria: *Betaproteobacteria* and *Zetaproteobacteria* are described in the phylum *Proteobacteria* [30]. Iron is necessary for the proliferation of microbial agents of infectious diseases that developed ways for iron acquisition from the host, while the host has protective mechanisms preventing iron acquisition by microorganisms [30,31].

In light of the presented facts, it is logical to ask whether NPs (IONPs) based on compounds of the biogenic element, which is so important for vital activities, can have a bactericidal effect. On the one hand, a negative answer is expected; however, several studies noticed the antimicrobial action of IONPs [32,33]. On the other hand, the bactericidal action was repeatedly confirmed for NPs based on other biogenic elements: ZnO and CuO, as was mentioned above.

Iron is like a double-edged sword. Despite its above-mentioned functions in living organisms, it is able to catalyze reactions of damaging DNA, lipids, and proteins by the Fenton reaction [34]. In this reaction, the free Fe^{2+} ion reacts with hydrogen peroxide (H_2O_2); as a result, a hydroxyl radical and Fe^{3+} ion are formed. The following reaction of Fe^{3+} with the superoxide anion radical ($\text{O}_2^{\cdot -}$) leads to the formation of molecular oxygen (O_2) and regeneration of Fe^{2+} as the initial catalyst. To protect it from the damage caused by the generation of hydroxyl radicals, it is necessary to maintain an extremely low level of free iron ions inside cells [35]. ROS generation is no single mechanism of antibacterial action of IONPs. A more detail description of these mechanisms is contained in Section 2.2.

The antibacterial properties are found both in nanoparticles based on iron oxides (IONPs) and in free iron ions; however, contrary to free ions, IONPs do not exert a significant toxic effect on mammalian cells [8,36,37]. Iron oxide nanoparticles can be obtained by different methods, from laser ablation to chemical synthesis [38–43]. It is assumed that the antibacterial properties of iron oxide nanoparticles are associated not only with the oxide form but, also, with the size, morphology, and other physicochemical properties of nanoparticles. Several types of iron oxides are known. The most frequently found are hematite Fe_2O_3 , magnetite Fe_3O_4 , and limonite $\text{Fe}_2\text{O}_3 \times \text{H}_2\text{O}$ [5,16].

Iron oxide nanoparticles (IONPs) have found wide applications in different fields of biomedicine—for example, in visualization and diagnostics [44]; in magnetic resonance imaging and computed tomography [45–48]; in positron emission tomography [49]; in cancer therapy with magnetic hyperthermia [50–52]; and for the separation of cells or molecules and the development of biosensors, which can applied to immunoassays, neuro-electronic studies, and biomedical imaging [53–56]. IONPs may be used in the imaging and tracking of brain cells in vivo [57]. A possibility of using iron oxide nanoparticles for delivering medicines and viral vectors to target cells is shown [58,59]. The antibacterial activity of iron oxide nanoparticles (IONPs) is of special interest, as the emergence of antibiotic-resistant strains is a serious problem for world public health. The direct bactericidal action of IONPs was described by the example of *S. aureus* [32]. Fe_3O_4 NPs can be used in regenerative medicine [60]. With that, IONPs have good biocompatibility in vivo and in vitro [61,62], which qualitatively distinguish IONPs from ZnO NPs having high cytotoxicity [63,64]. The balance of the antimicrobial activity and biocompatibility makes IONPs an attractive candidate for the role of an antimicrobial preparation of the new generation. The present review is intended to inform readers about available data on the antibacterial properties of IONPs, a range of susceptible bacteria, mechanisms of the antibacterial action, the dependence of the antibacterial action of IONPs on the method for synthesis, and the biocompatibility of IONPs with eukaryotic cells and tissues.

2. Main Part

2.1. Susceptible Microorganisms

A list of microorganisms susceptible to the toxic action of IONPs is presented in Table 1. A minimum of 10 species of Gram-negative and 11 species of Gram-positive bacteria, as well as three fungal species susceptible to IONPs, have been mentioned in the

literature (Table 1). The majority of the indicated microorganisms have epidemiological significance [65]. A range of the bacteriostatic concentrations for IONPs is quite wide and makes up 25–2000 µg/mL.

Table 1. List of the microorganisms susceptible to the toxic action of IONPs.

Group of Microorganism	Species/Serotype	Reference
Gram-negative bacteria	<i>Escherichia coli</i>	[33,66–80]
	<i>Klebsiella pneumoniae</i>	[70,72,74,77,80–82]
	<i>Klebsiella</i> sp.	[36]
	<i>Proteus mirabilis</i>	[73]
	<i>Proteus vulgaris</i>	[83]
	<i>Pseudomonas aeruginosa</i>	[71,79,80,82,84–86]
	<i>Salmonella enterica</i> serotype typhimurium	[76,81,87]
	<i>Serratia marcescens</i>	[32,71]
	<i>Vibrio cholerae</i>	[8]
	<i>Xanthomonas</i> sp.	[83]
Gram-positive bacteria	<i>Bacillus brevis</i>	[8]
	<i>Bacillus cereus</i>	[87]
	<i>Bacillus licheniformis</i>	[8]
	<i>Bacillus</i> sp.	[36]
	<i>Bacillus subtilis</i>	[8,70,72,73,76,78,79]
	<i>Corynebacterium</i> sp.	[75]
	<i>Enterococcus hirae</i>	[66]
	<i>Listeria monocytogenes</i>	[71,87]
	<i>Micrococcus luteus</i>	[67]
	<i>Staphylococcus aureus</i>	[8,33,36,67–70,72,74,76,77,79–81,85,86]
Fungi	<i>Staphylococcus epidermidis</i>	[8,88,89]
	<i>Streptococcus mutans</i>	[8,88,89]
	<i>Aspergillus niger</i>	[90]
	<i>Candida albicans</i>	[87,90]
	<i>Candida glabrata</i>	[87]
	<i>Candida glochares</i>	[87]
	<i>Candida saitoana</i>	[87]
	<i>Fusarium solani</i>	[90]

IONPs have antimicrobial activity against both Gram-positive (including *Staphylococcus aureus*) and Gram-negative (including *Escherichia coli*) bacteria [33]. The data about the dependence of the antibacterial action of IONPs on the bacterial group (Gram-positive or Gram-negative) are ambiguous. On the one hand, there are data about the comparable effects of IONPs against Gram-negative and Gram-positive bacteria [91], similar to CuO [92], which distinguishes IONPs from ZnO NPs [93]. On the other hand, there are data about the more pronounced bacteriostatic action of Fe₃O₄ against Gram-negative bacteria compared to Gram-positive [66]. The authors linked the indicated differences with the peculiarities of the cell wall structure and metabolism of Gram-positive and Gram-negative bacteria [66].

2.2. The Mechanisms of Antibacterial IONP Activity

One of the main mechanisms of IONP toxicity is ROS generation [5,94], including in photocatalysis, Fenton reactions, or similar ones [88]. ROS, in turn, have a genotoxic action, damaging DNA molecules (Figure 1) [94]. An increase in ROS concentration can be caused by a decrease in the activity of antioxidant system enzymes (SOD, catalase, and glutathione reductase) [67]. Metal ions are able to bind mecapto (–SH), amino (–NH), and carboxyl (–COOH) groups of proteins, including enzymes, which leads to inactivation or partial inhibition [95]. Additionally, IONPs damage the bacterial cell wall integrity, as shown in reference [94]. The direct binding of IONPs with the cell wall of *Staphylococcus*

aureus was shown by scanning electron microscopy [96]. IONPs can cause a decrease in the expression of antibiotic resistance genes (ARGs) in antibiotic-resistant bacteria found in operating rooms [5]. IONPs are able to disturb the function of F_0/F_1 -ATPase and reduce the rate of H^+ flow through the membrane and the redox potential [66]. The mechanisms of the antimicrobial action for IONPs have been suggested in several studies based on their size and are common for other types of metal oxide nanoparticles [95,97]. An ability to inhibit DNA replication by the inactivation of topoisomerase is described for nanoparticles with small sizes [98]. It was shown by the method of electron microscopy that Fe_2O_3 NPs can bind directly with the cell wall of *E. coli*. IONPs can also penetrate into the cytoplasm, concentrate in it, and cause vacuole formation and cell wall disruption [84,99].

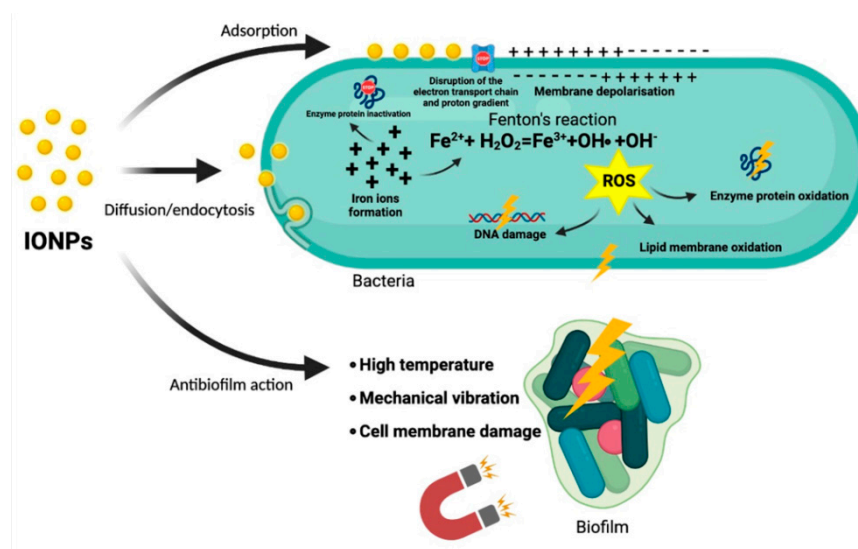


Figure 1. The mechanisms of IONP antibacterial activity.

Fe_3O_4 IONPs can concentrate between the outer and inner membranes of the cell wall in Gram-negative bacteria due to binding with the FHL complex in the inner membrane. Therefore, Fe_3O_4 IONPs have more pronounced antimicrobial actions against Gram-negative bacteria [66].

Bactericidal and antibiofilm activities were shown in Fe_3O_4 IONPs. Positively charged and neutral IONPs promoted a higher reduction of *Streptococcus mutans* biofilms compared with negatively charged IONPs [89]. IONPs coated with oleic acid can prevent biofilm formation by *S. aureus* and *P. aeruginosa* [85]. IONPs have the ability to adsorb and penetrate into bacterial biofilms due to their physicochemical characteristics, such as a surface charge, hydrophobicity, and high surface area ratio by volume [100,101].

Iron oxide nanoparticles have both magnetic and paramagnetic properties [68,87,102]. Fe_3O_4 NPs with high paramagnetic activity are also named superparamagnetic iron oxide nanoparticles (SPIONs) [103,104]. SPIONs in the presence of the alternating magnetic fields cause cell death and biofilm destruction due to the vibration damage, local hyperthermia, and ROS generation. All of the above-mentioned factors lead to the dissociation of bacteria from a biofilm, damage of the bacterial cell wall, membrane rupture, the fusion of different cells with each other, and death [69].

In 80% of studies, IONPs show only bacteriostatic action. The bactericidal action of IONPs is described in the literature in 20% of cases.

2.3. Methods of IOPNs Synthesis

The methods for IONP synthesis are multiple and include coprecipitation [105], thermal decomposition [70], low temperature synthesis [71], the sol-gel method [106], hydrothermal method [69], electrochemical method [83], laser ablation [91,107], sonochemical, microwave, microemulsion methods, matrix-mediated method using PVA, “green synthe-

sis" [68], and many others [32,84,108]. In the case of research of IONP antibacterial effects, most used in coprecipitation, thermal decomposition, the sol–gel method, laser ablation, and "green synthesis" (Table 2); therefore, we shall briefly describe these methods below.

Aqueous coprecipitation is the most widely used chemical method of IONP synthesis [105,109]. In this method, IONPs are synthesized by the simultaneous precipitation of Fe^{2+} and Fe^{3+} salts (molar ratio 1:2) in a basic solution at room temperature or under heat [105,109,110]. The advantage of the coprecipitation method is the low cost of IONPs synthesis. It is important in cases of large-scale production [27]. The disadvantages of the method are the large size distribution of produced IONPs, aggregation, poor crystallinity, a high possibility of oxidation, and poor magnetic property [111]. The change of pH in the solution can improve the properties of IONPs synthesized by coprecipitation [112].

The thermal decomposition is a nonaqueous synthesis in which organometallic compounds such as $\text{Fe}(\text{Acac})_3$, $\text{Fe}(\text{C}_2\text{O}_4) \times 2 \text{H}_2\text{O}$, $\text{Fe}(\text{CH}_3\text{COO})_2$, or ferrocene suffer decay at high temperatures in organic solvents (high boiled) or via being solvent-free in the presence of stabilizing surfactants like aliphatic amine and fatty acids [113]. This method may generate high-quality IONPs with close distributions of particle sizes and a high magnetism and degree of crystallinity [113]. Additional advantages of this method are the high yield and absence of IONP aggregation [114]. The main disadvantage of this method is the insolubility of produced IONPs in water. Therefore, further steps are required to make their surfaces hydrophilic and use IONPs in biological solutions [115].

The sol–gel method (wet–chemical method) is a sum of reactions of condensation and hydrolysis between iron alkoxides and salts (e.g., chlorides, nitrates, and acetates) [116]. The main advantage of this method is a good homogeneity and size and high purity and quantity of IONPs [116]. The disadvantages of the method are the requirements for compliance with exact values of the pH, temperature, and concentration of the reagents during a synthesis; high cost of precursors; and low wear resistance of synthesized IONPs [117].

Laser ablation synthesis in a solution is a synthesis that is triggered by the immersion of pulsed laser beams on the target material in a liquid solution [118]. Laser ablation synthesis allows to work with a wide range of materials and solvents. The size and clustering of IONPs are difficult to control [118]. Laser ablation allows the synthesis of FeOx crystal to a few atom clusters in the following modification: phosphonates as an aqueous solution and bulk iron as a target [72].

The so-called "green synthesis" has aroused considerable interest. It is a modification of synthesis methods (as a rule, coprecipitation) with the application of plant extracts used as a reducing agent. There are reports about the application of leaf extracts of *Psidium guajava* [68], *Cynometra ramiflora* [88], *Sida cordifolia* [119], *Zea mays* [87], *Argemone mexicana* [73], *Couroupita guianensis* [81], *Tridax procumb* [120], peel extracts of *Punica granatum* [70], *Ruellia tuberosa* [74], *Malva sylvestris* [82], and *Citrus sinensis* [121]. This method is low-cost, if coprecipitation is used as a basic technique [74,82,121].

Large-scale synthesis is a modification of the coprecipitation method with controlled heating and addition polyacrylic acid salts or sodium oleate as the surfactant [103]

The hydrothermal method is a synthesis of IONPs from iron precursors at high pressure and temperature conditions in an aqueous medium [103,104]. Aqueous synthesis methods generate particles with low crystallization [122]. Replacing water with other organic solvents allows the formation of IONPs with high crystallinity and controlled shapes. This method is named solvothermal synthesis [113]. The disadvantage of this method is the long time it takes for synthesis (hours to days) [123].

2.4. Dependence of the Antimicrobial Action of IONPs on the Size and Type of Iron Oxides

The majority of studied IONPs have a spherical shape (Table 2), which excludes a contribution of the shape into the antimicrobial action. Therefore, we assessed the sizes and compositions of IONPs. Based on the analyzed literature data, we did not reveal an association between the IONPs' size and the minimum bacteriostatic concentrations (Figure 2a). Several IONP types are distinguished depending on the oxide on which

basis they are synthesized: NPs based on hematite (α -Fe₂O₃) [5,68], β -Fe₂O₃, γ -Fe₂O₃, ϵ -Fe₂O₃ [124–126], and Fe₃O₄ [83,127]. We found that Fe₂O₃ NPs show more pronounced bacteriostatic actions compared to Fe₃O₄ NPs (Figure 2b). For more detailed analyses, we assessed the contribution of a method for IONP synthesis of their antimicrobial properties.

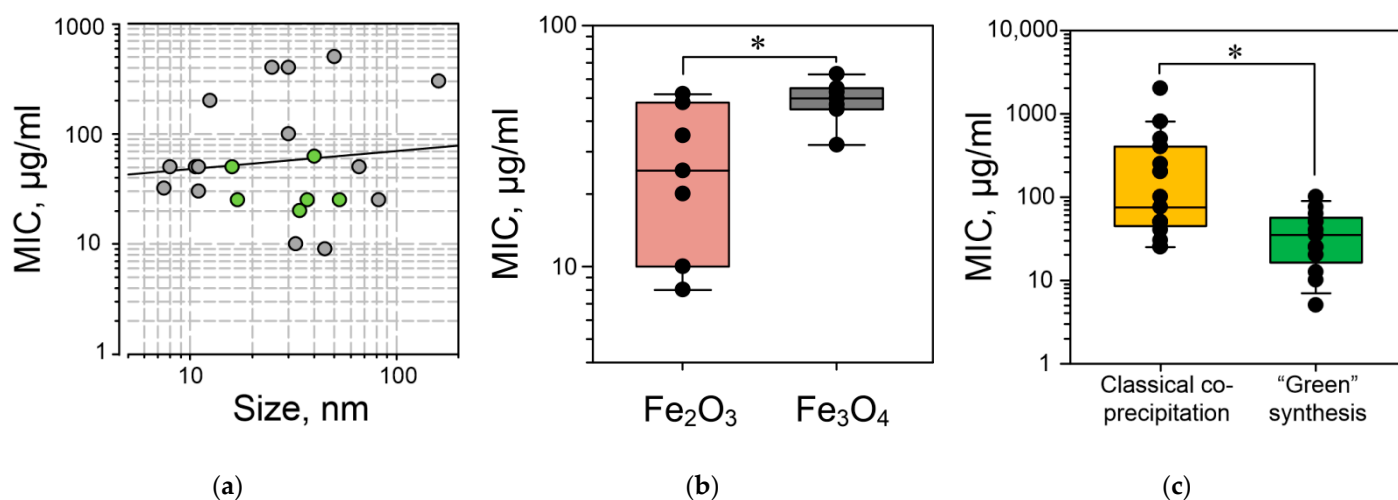


Figure 2. (a) Assessment of the dependence of the IONP MIC against *E. coli* on the IONP size. (b) Assessment of the dependence of the IONP MIC against *E. coli* on the iron oxide type. (c) Assessment of the dependence of the IONP MIC against *E. coli* in the synthesis method. Values of the minimum inhibitory concentrations are taken from the sources in Table 2. In (a), the grey color shows the values for the IONPs obtained without “green synthesis”, and the green color shows the values for the IONPs obtained by “green synthesis”. *— $p < 0.05$ by the Mann–Whitney *U* test.

2.5. Dependence of the Antimicrobial Action of IONPs on a Synthesis Method

The methods for IONPs synthesis are multiple and include coprecipitation [105], thermal decomposition [70], low-temperature synthesis [71], the sol–gel method [106], hydrothermal method [69], electrochemical method [83], laser ablation [91,107], sonochemical, microwave, microemulsion methods, matrix-mediated method using PVA, and many others [32,84,108]. IONPs synthesized by the low-temperature method from iron sulfate showed an antimicrobial effect against *E. coli*, *P. aeruginosa*, *Serratia marcescens*, and *Listeria monocytogenes*, exerting bacteriostatic action and inhibiting biofilm formation [71]. NPs obtained by laser ablation had comparable bacteriostatic effects against Gram-negative (*Escherichia coli*, *Pseudomonas aeruginosa*, and *Serratia marcescens*) and Gram-positive (*Staphylococcus aureus*) bacteria. The bacteriostatic actions of IONPs do not depend on a solvent (SDS or DMF) or bacterial group (Gram-positive or Gram-negative) [91].

2.5.1. Coprecipitation Method

The most common method for IONP synthesis when studying the antimicrobial properties is the coprecipitation of salts Fe³⁺/Fe²⁺ [56,73,75,86,127–129]. This synthesis method is the most available. Modifications of the method are possible. For instance, the addition of oleic acid for the generation of conjugated IONPs [127,129], as well as the coprecipitation of different metal salts, allow us to obtain composite NPs—for example, based on FeSO₄ × 7 H₂O and Co(NO₃)₂ × 6 H₂O [76]. One of the methods for improving the antimicrobial properties of IONPs is the use of composites—for example, α -Fe₂O₃/Co₃O₄ [105]. Composite NPs have more pronounced antimicrobial actions against *B. subtilis*, *S. aureus*, *E. coli*, and *S. typhimurium*. The synergistic effect of Fe₂O₃ and Co₃O₄ was observed compared to oxides used individually. However, upon the strong bacteriostatic action (practically a full inhibition of the bacterial growth at a concentration of 1200 mg/mL), the bactericidal action was almost absent [76]. α -Fe₂O₃/ZnO NPs show more pronounced bacteriostatic actions against Gram-positive *Bacillus subtilis* and *Staphylococcus aureus* and

Gram-negative *Escherichia coli* and *Salmonella typhi* than IONPs and ZnO NPs; with that, the size of the inhibition zone increases when the ZnO concentration in the composite is increased [76], (Table 2).

Compared to Fe₃O₄ NPs, the composite Fe₃O₄/SiO₂ NPs has a more pronounced photocatalytic bactericidal action against *Escherichia coli* and *Staphylococcus aureus*; with that, the effect was higher against Gram-positive bacteria [130]. The use of the combined method for IONPs synthesis allows achieving a significant bacteriostatic effect against *Staphylococcus aureus*, *Xanthomonas*, *Escherichia coli*, and *Proteus vulgaris* [83].

2.5.2. “Green Synthesis”

The so-called “green synthesis” has aroused considerable interest. It is a modification of synthesis methods (as a rule, coprecipitation) with the application of plant extracts used as a reducing agent [83,106–110].

IONPs synthesized by the “green” method show comparable antimicrobial effects against both Gram-negative (*E. coli*) and Gram-positive (*S. aureus*) bacteria [68]. However, the antimicrobial effect of 50–100 µg/µL of IONPs is about three times lower than that of 20 µg/mL of streptomycin. IONPs synthesized in the presence of *Punica granatum* peel extract exert a bacteriostatic effect on *Pseudomonas aeruginosa*; with that, these IONPs do not have hemolytic activity against erythrocytes [70]. IONPs in complex with *Cynometra ramiflora* extract have more pronounced bacteriostatic effects against Gram-positive *S. epidermalis* compared to Gram-negative *E. coli* [88]. NPs synthesized in the medium of the *Zea mays* extract did not have their own antimicrobial and antifungal properties but significantly enhanced the bacteriostatic action of kanamycin and rifampicin against Gram-positive *Bacillus cereus*, *Listeria monocytogenes*, and *Staphylococcus aureus* and Gram-negative *Escherichia coli* and *Salmonella typhimurium*, as well as the antifungal activity these antibiotics against six strains of *Candida* [87]. In addition to the antimicrobial properties, IONPs obtained as a result of “green” synthesis had antioxidant properties and inhibited their proteasome activity, which allowed us to regard IONPs as possible candidates for cancer therapy [87].

Compared to Fe₃O₄ NPs, Fe₃O₄/*Malva sylvestris* NPs had more pronounced bacteriostatic and bactericidal effects against *Staphylococcus aureus*, *Corynebacterium* sp., *Pseudomonas aeruginosa*, and *Klebsiella pneumoniae* and exerted cytotoxic action against the Hep-G2 and MCF-7 cell lines [82].

IONPs synthesized in the *Argemone mexicana* extract had more pronounced bacteriostatic activity against *E. coli*, *P. mirabilis*, and *B. subtilis* than pure IONPs, which was comparable with the effects of streptomycin [73].

Table 2. Parameters of the nanoparticles reported in the literature.

Nº	Synthesis Method	Composition	Size, nm	Shape	Concentration	Medium, Conditions	Microorganism	Biological Effect	Ref
1	Coprecipitation method	Fe ₂ O ₃	25–40	Sph	10–50 µg/mL	NA, 48 h, 37 °C	<i>E. coli</i> , <i>S. aureus</i> , <i>S. dysenteriae</i>	BS	[33]
2	Chemical precipitation using <i>Psidium Guajava</i> leaf extract as a reducing agent followed by heat treatment	Fe ₂ O ₃	34	Sph	20–100 µg/mL	MHA, 24 h, 37 °C	<i>E. coli</i> , <i>S. aureus</i>	BS	[68]
3	Chemical precipitation using <i>Punica granatum</i> peel extract as a reducing agent followed by heat treatment	-	-	-	31 µg/mL	MHA, 24 h, 37 °C	<i>P. aeruginosa</i>	BS	[70]
4	Wet chemical method	Fe ₃ O ₄	33–40	Sph	25–100 µg/mL	NA, 24 h, 37 °C	<i>E. coli</i> , <i>P. vulgaris</i> , <i>S. aureus</i> , <i>Xanthomonas</i> sp.	BS	[83]
5	Modified coprecipitation method	Fe ₃ O ₄	10.64 ± 4.73	Sph	50–500 µg/mL	NA, 24 h, 3 °C	<i>E. coli</i> , <i>E. hirae</i>	BS	[66]
6	Coprecipitation	α-Fe ₂ O ₃ /Co ₃ O ₄ composite	25	Rod/ hexag	400–800 µg/mL	MHA, 24 h, 37 °C	<i>B. subtilis</i> , <i>E. coli</i> , <i>S. aureus</i> , <i>S. typhimurium</i> .	BC	[76]
7	Chemical precipitation using <i>Cynometra ramiflora</i> extract as a reducing agent	Fe ₂ O ₃ /Fe ₃ O ₄	-	Sph	70 µL of IONPs suspension/disk	NA, 24 h, 37 °C	<i>E. coli</i> , <i>S. epidermidis</i>	BS	[88]
8	Coprecipitation method	α-Fe ₂ O ₃ , ZnO/α-Fe ₂ O ₃	~30	Sph/oval	400–800 µg	MHA, 24 h, 37 °C	<i>B. subtilis</i> , <i>E. coli</i> , <i>S. aureus</i> , <i>S. typhimurium</i>	BS	[76]

Table 2. Cont.

№	Synthesis Method	Composition	Size, nm	Shape	Concentration	Medium, Conditions	Microorganism	Biological Effect	Ref
9	Coprecipitation method	Fe ₃ O ₄	6–9	Sph	32–128 µg/mL	LB broth, 37 °C	<i>E. coli</i> , <i>L. monocytogenes</i> , <i>P. aeruginosa</i> , <i>S. marcescens</i>	BS	[71]
10	Chemical precipitation using <i>Sida cordifolia</i> as a reducing agent and stabilizer	Fe ₂ O ₃	16	Sph	50 µg/mL	MHA, 24 h, 37 °C	<i>B. subtilis</i> , <i>E. coli</i> , <i>K. pneumoniae</i> , <i>S. aureus</i>	BS	[119]
11	Coprecipitation method	IONPs with amoxicillin	-	-	0.05–10 mM	TSB, 24 h, 37 °C	<i>P. aeruginosa</i> , <i>S. aureus</i>	Stimulation of bacterial growth in the presence of humic acid	[86]
12	Ready commercial product (Sigma-Aldrich)	Fe ₂ O ₃	<5	-	0.05–10 mM	LB, 37 °C	<i>E. coli</i>	BC	[99]
13	Coprecipitation using the aqueous extract of corn (<i>Zea mays</i> L.) ear leaves	Fe ₃ O ₄	37.86	Sph	25–50 µg/disc	NB, 37 °C at 24 h, for bacteria, PDA, 28 °C at 48 h for fungi	<i>B. cereus</i> , <i>C. albicans</i> , <i>C. glabrata</i> , <i>C. geochares</i> , <i>C. saitoana</i> , <i>E. coli</i> , <i>L. monocytogenes</i> , <i>S. aureus</i> , <i>S. typhimurium</i> ,	BS	[87]
14	Coprecipitation method in alkaline media with leaf extract of <i>A. mexicana</i>	Fe ₃ O ₄	10–30	Sph	12.5–50 mg/disc	MHB, 24 h, 37 °C	<i>B. subtilis</i> , <i>E. coli</i> , <i>P. mirabilis</i> ,	BS	[73]
15	Laser ablation in dimethylformamide (DMF) and sodium dodecyl sulfate (SDS) solutions	α-Fe ₂ O ₃	50–110	Sph	4.25 mg/mL	NA, 24 h, 37 °C	<i>E. coli</i> , <i>P. aeruginosa</i> , <i>S. aureus</i> , <i>S. marcescens</i>	BS	[91]

Table 2. Cont.

Nº	Synthesis Method	Composition	Size, nm	Shape	Concentration	Medium, Conditions	Microorganism	Biological Effect	Ref
16	Coprecipitation using <i>Couroupita guianensis</i> aqueous fruit extract	Fe ₃ O ₄	~17	Sph	25–75 µg/mL	NA, 24 h, 37 °C	<i>E. coli</i> , <i>K. pneumoniae</i> , <i>S. typhimurium</i>	BS	[81]
17	Coprecipitation	Fe ₃ O ₄ coated by SiO ₂	~20	Sph	-	NA, 24 h, 37 °C	<i>E. coli</i> , <i>S. aureus</i> ,	BS	[130]
18	Chemical precipitation using <i>Tridax procumbens</i> leaf extract as a reducing agent	Fe ₃ O ₄	-	Sph	10–40 µL	PDA	<i>P. aeruginosa</i>	BS	[120]
19	Coprecipitation	Fe ₃ O ₄	8	Sph	50–200 µg/mL	LB, 37 °C, 14 h	<i>E. coli</i>	BS	[75]
20	Ultra-large-scale synthesis	Fe ₃ O ₄ or Fe ₃ O ₄ coated by alginate	~16, for coated with alginate ~230	Sph	2.5–10 µg	LB, 37 °C, 16–18 h	<i>P. aeruginosa</i>	BS	[95]
21	Chemical precipitation using <i>Ruellia tuberosa</i> leaf aqueous extract as a reducing agent	FeO	52.78	Rod	25–75 µg/mL	MHA, 24 h, 37 °C,	<i>E. coli</i> , <i>K. pneumoniae</i> , <i>S. aureus</i>	BS	[74]
22	Coprecipitation	PEG-Fe ₃ O ₄	26 ± 1.26	Sph	0.1–100 µg/mL	-	<i>E. coli</i> , <i>M. luteus</i> , <i>S. aureus</i> ,	BS	[67]
23	Coprecipitation using <i>Malva sylvestris</i> as a reducing agent	Fe ₃ O ₄	30–50	Sph	62.5 mg/mL	BHI, 24 h, 37 °C,	<i>Corynebacterium</i> sp., <i>K. pneumoniae</i> , <i>P. aeruginosa</i> , <i>S. aureus</i> ,	BS, BC	[82]
24	One-pot hydrothermal method	Fe ₃ O ₄	~160	Sph	300–1000 µg/mL	LB, 37 °C, 14 h	<i>E. coli</i> , <i>S. aureus</i>	BS	[69]
25	Chemical precipitation using orange peel extract as a reducing and stabilizing agent	Fe ₂ O ₃	~50	-	0.5 mg/mL	NA, 36 °C, 24 h	<i>B. subtilis</i> , <i>E. coli</i> , <i>P. aeruginosa</i> , <i>S. aureus</i>	BS	[121]

Table 2. Cont.

№	Synthesis Method	Composition	Size, nm	Shape	Concentration	Medium, Conditions	Microorganism	Biological Effect	Ref
26	Chemical precipitation using <i>Urtica</i> leaf extract as a reducing agent	α -Fe ₂ O ₃ , α -Fe ₂ O ₃ -Ag	100–200	Different	35 μ g/mL 5–35 μ g/disc	MHA, 24 h, 37 °C,	<i>Bacillus sp.</i> , <i>E. coli</i> , <i>K. pneumoniae</i> , <i>S. aureus</i> <i>E. coli</i> DH5 α -pUC18 ampicillin-resistant;	BS	[36]
27	Coprecipitation	Fe ₃ O ₄	10.64 \pm 4.73	Sph	50–250 μ g/mL	Peptone medium, 24 h, 37 °C,	<i>E. coli</i> pARG-25 kanamycin-resistant	BS	[66]
28	Coprecipitation	Fe ₃ O ₄	10–120	Sph	50 mg/mL	NA, 24 h, 37 °C,	<i>B. brevis</i> , <i>B. licheniformis</i> , <i>B. subtilis</i> , <i>E. coli</i> , <i>P. aeruginosa</i> , <i>S. aureus</i> , <i>S. epidermidis</i> , <i>S. flexneri</i> , <i>V. cholera</i>	BS	[9]
29	Coprecipitation	Fe ₃ O ₄ , Co/Fe ₂ O ₄ , Mn/Fe ₂ O ₄	14–68	Cubic spinel	25–2000 μ g/mL	NB, NA, 24 h, 37 °C,	<i>B. subtilis</i> , <i>E. coli</i>	BS	[102]
30	Solvothermal method	IONPs modified with oleic acid	75–1110	Sph	25–125 μ g/mL	LB broth, 48 h, 37 °C,	<i>P. aeruginosa</i> , <i>S. aureus</i>	BS	[85]
31	Laser ablation in dimethylformamide (DMF) and sodium dodecyl sulfate (SDS) solutions	α -Fe ₂ O ₃	50–110	Sph	-	NA, 24 h, 37 °C,	<i>E. coli</i> , <i>P. aeruginosa</i> , <i>S. aureus</i> , <i>S. marcescens</i>	BS	[91]

Table 2. Cont.

№	Synthesis Method	Composition	Size, nm	Shape	Concentration	Medium, Conditions	Microorganism	Biological Effect	Ref
32	Sol-gel combustion	Fe ₂ O ₃	35.16 ± 1.47	Sph	65 ± 1.5 µg/mL	MHB, 24 h, 35 ± 2 °C,	<i>B. subtilis</i> , <i>E. coli</i> , <i>P. aeruginosa</i> , <i>S. aureus</i>	Low BC	[13]
33	Matrix-mediated method using PVA (polyvinyl acetate)	Fe ₃ O ₄ /Fe ₂ O ₃	9 ± 4	Sph	30–3000 µg/mL,	TSB, 24 h, 37 °C,	<i>S. aureus</i>	BS, BC	[32]
34	Laser ablation in the water	IONPs/carbon nanotubes	6–7	Sph IO on the carbon nanotubes	400–800 µg/mL	NB, 24 h, 37 °C,	<i>E. coli</i> , <i>K. pneumoniae</i> , <i>S. aureus</i>	BS	[77]
35	Coprecipitation	Fe ₃ O ₄ conjugated with TEPSA or TPED	14.6 ± 1.4, 20.4 ± 1.3 or 21.2 ± 1.6	Sph	1–3 µg/mL	TYE, 24 h, 37 °C, in the dark	<i>Streptococcus mutans</i>	BC	[89]
36	Coprecipitation	Fe ₃ O ₄ coated by citric acid	~30	Sph	100 µg/mL	NA, 24 h, 37 °C,	<i>E. coli</i> , <i>S. typhimurium</i>	BS	[131]
37	Coprecipitation method	Fe ₃ O ₄ , Fe ₂ O ₃ coated by chitosan	10–20	Sph	2.5–50 µM	NB, 37 °C	<i>B. subtilis</i> , <i>E. coli</i>	BC	[78]
38	Coprecipitation	Fe ₃ O ₄ coated by chitosan	~11	Sph	30–40 µg/mL	TSA for bacteria, YEPD for <i>C. albicans</i> , CYA for <i>A. niger</i> , Potato sucrose agar for <i>F. solani</i> . 48 h at 30 °C	<i>A. niger</i> , <i>B. subtilis</i> , <i>C. albicans</i> , <i>E. coli</i> , <i>F. solani</i>	BS	[90]
39	Coprecipitation method	Fe ₂ O ₃ , FeO, coated by gentamicin	10–15	Sph	200 µg/mL	LB broth, 24 h, 37 °C	<i>B. subtilis</i> , <i>E. coli</i> , <i>P. aeruginosa</i> , <i>S. aureus</i>	BC	[79]
40	Coprecipitation	Fe ₃ O ₄	20–25	-	5–80 µg/mL	NB, 24 h, 37 °C	<i>B. cereus</i> , <i>K. pneumoniae</i> ,	BS, BC	[132]

Table 2. Cont.

Nº	Synthesis Method	Composition	Size, nm	Shape	Concentration	Medium, Conditions	Microorganism	Biological Effect	Ref
41	Coprecipitation using <i>Glycosmis mauritiana</i> water extract as a reducing agent	Fe ₃ O ₄	<100	Sph	10–30 µg/µL	MHA, 24 h, 37 °C,	<i>E. coli</i> , <i>K. pneumoniae</i> , <i>P. aeruginosa</i> , <i>S. aureus</i>	BS	[80]

BHI—Brain heart infusion, BS—bacteriostatic effect, BC—bactericidal effect, Hexag—hexagonal, IONPs—iron oxide nanoparticles, LB—lysogeny broth, MHA—Mueller–Hinton Agar, NA—Nutrient Agar, NB—Nutrient broth, PDA—Potato dextrose agar, Rod—rod-shaped, Sph—spherical, TEPsA—3-(triethoxysilyl) propylsuccinic anhydride, TPEd—N-[3-(trimethoxysilyl)propyl] ethylenediamine, TSB—Tryptic soy broth, YEA—Czapek yeast extract agar, and YEPD—yeast extract peptone dextrose.

Fe₃O₄ NPs synthesized with a *Couroupita guianensis* extract inhibited the growth of *E. coli*, *S. typhimurium*, *K. pneumoniae*, and *S. aureus* and induced the apoptosis of the hepatocellular carcinoma (HepG2) cell line [81]. IONPs synthesized in a *Ruellia tuberosa* extract inhibited the growth of *E. coli*, *K. pneumoniae*, and *S. aureus* in a dose-dependent manner. The IONP effectiveness turned to be higher than that of streptomycin. The mechanism of antimicrobial action is the photocatalytic generation of ROS [74]. Fe₂O₃/*Citrus sinensis* NPs exerted a comparable bacteriostatic action against Gram-positive (*B. subtilis* and *S. aureus*) and Gram-negative (*E. coli* and *P. aeruginosa*) bacteria. The inhibitory effect of Fe₂O₃/*Citrus sinensis* NPs was comparable with chlorhexidine, hexachlorophene, benzalkonium chloride, and phenol taken in equal concentrations [121]. α-Fe₂O₃ NPs, in combination with a *Sida cordifolia* extract, had comparable bacteriostatic activity against *E. coli*, *K. pneumoniae*, *B. subtilis*, and *S. aureus*. The bacteriostatic effect against Gram-positive bacteria was more strongly pronounced and was comparable with the effect of neomycin [119]. Unfortunately, for several extracts—for example, *Couroupita guianensis*—“green synthesis” leads to an enhancement of IONP cytotoxicity [81]. In another study, the antioxidant properties were described for Fe₃O₄ NPs synthesized by the “green method” [87]. In a meta-analysis, we found that IONPs generated by the “green synthesis” method had three times more pronounced bacteriostatic activity than IONPs generated by the coprecipitation method (Figure 2c).

2.6. Additional Methods for Increasing the Antimicrobial Activity of IONPs

Iron oxide nanoparticles have both magnetic and paramagnetic properties [68,87,102–104]. The use of an alternating magnetic field allows additional increases in the bactericidal action of Fe₃O₄ NPs against *E. coli* and *S. aureus*, causing cell death and biofilm destruction due to the photocatalytic generation of ROS, and local hyperthermia and vibration damage occurred under the action of the magnetic field. All of the above-mentioned factors lead to the dissociation of bacteria from the biofilm, damage of the bacterial cell wall, membrane rupture, the fusion of different cells with each other, and death [69].

Fe₂O₄ composite NPs with the addition of different ratios of Co and Mn have magnetic properties due to Fe₂O₄ and inhibit the growth of *E. coli* and cause damage to *E. coli* and *B. subtilis* in a dose-dependent manner [102].

IONP conjugation with carbon nanotubes allows achieving a bactericidal effect against Gram-negative (*E. coli* and *K. pneumoniae*) and Gram-positive (*Staphylococcus aureus*) bacteria; with that, the CFU were reduced by two and more times compared to the control [77]. Carbon nanotubes/IONPs accelerated wound healing in mice in a wound-healing test by 25% and 50% compared to IONPs or carbon nanotubes taken individually. It is worth noting that, in this study, the size of the inhibition zone increased insignificantly upon a considerable decrease in the CFU; therefore, the antimicrobial effect of IONPs assessed by a size of the inhibition zone in the majority of studies can be underestimated. In contrast to other IONPs types, Fe₃O₄ IONPs coated with oleic acid exert a different effect on the growth and viability of Gram-positive (*Enterococcus hirae*) and Gram-negative (*E. coli*) bacteria. More pronounced antimicrobial action was observed against Gram-negative bacteria [127]. The authors linked this phenomenon with differences in the cell wall structure; in particular, with the ability of Fe₃O₄ IONPs to concentrate between the outer and inner membranes of the cell wall in Gram-negative bacteria and the presence of the FHL complex in the inner membrane of *E. coli*, which is an additional target for IONP Fe₃O₄. Fe₃O₄ NPs covered with oleic acid cause a reduction in the growth of kanamycin- and ampicillin-resistant *E. coli* strains due to retardation of the logarithmic growth phase, lag phase extension, reduction of the H⁺ flow through the membrane, and redox potential [85,131]. IONPs coated with oleic acid not only inhibit the growth of *S. aureus* and *P. aeruginosa* but also prevent biofilm formation [131].

Surface modification is also a key way to improve IONP the antibacterial properties [78]. The conjugation of IONPs with chitosan enhanced the bactericidal action of IONPs against *Bacillus subtilis* and *Escherichia coli* due to ROS generation [78].

Fe₃O₄ NPs covered with polyethylene glycol (PEG) exert a dose-dependent bactericidal action against the *E. coli* and *S. aureus* and antibiotic-resistant *Micrococcus luteus* strain. The mechanism of toxicity resides in a decrease in the activity of the antioxidant system enzymes (SOD, catalase, and glutathione reductase) and, as a consequence, enhancement of ROS generation and lipid oxidation [67].

Fe₃O₄ NPs conjugated with chitosan have bactericidal and fungicidal actions against *Candida albicans*, *Aspergillus niger*, and *Fusarium solani* [90]. Coating with alginate or tobramycin did not have a significant effect on the bacteriostatic activity of Fe₃O₄ NPs against *P. aeruginosa* [84].

Conjugation with polyethylene glycol (PEG) and chitosan allows not only improving the antimicrobial properties of IONPs but also reducing the undesirable adsorption of IONPs on liver macrophages [133,134].

One of the methods for improving the antimicrobial properties is the use of a combination of “green synthesis” and a change in the NP compositions—for example, the addition of gold. The bacteriostatic effect of the mixture *Urtica*/α-Fe₂O₃•Ag NPs against *S. aureus*, *Bacillus* sp., *Klebsiella* sp., and *E. coli* was higher compared to *Urtica*/α-Fe₂O₃ NPs. An increase in the inhibition zone was proportional to the silver concentration in the composite. Both *Urtica*/α-Fe₂O₃•Ag NPs and *Urtica*/α-Fe₂O₃ NPs had more pronounced effects on the growth of the Gram-negative strains [36]. Some of the mechanisms of action of Fe₃O₄ and Ag NPs are membrane damage, a decrease in the redox potential, and H⁺ fluxes, which lead to the inhibition of the activity of bacterial F₀/F₁-ATPase [131].

The combined use of NPs from iron oxides and gold does not reduce the growth of the bacterial biomass of the *E. coli* culture but prevents bacterial cell division [75]; as a consequence, *E. coli* alters their morphology from rods to filaments with a length of several micrometers. The mixture of Fe₃O₄ and Au NPs inhibits the growth of the kanamycin-resistant *Escherichia coli* and *Salmonella typhimurium* strains more effectively than Fe₂O₃ NPs [75].

An approach to an improvement in the antimicrobial properties of IONPs by their conjugation with antibiotics is described by the example of gentamicin [79]. With that, a more pronounced bacteriostatic effect was achieved against Gram-positive *B. subtilis* and *S. aureus* than Gram-negative *E. coli* and *P. aeruginosa*. A conjugation with gentamicin reduced the minimum inhibitory concentration against all indicated strains by more than ten times [79]. In several cases, the conjugation of IONPs with antibiotics can give an opposite result. IONPs conjugated with amoxicillin enhanced the growth of *Pseudomonas aeruginosa* and *Staphylococcus aureus* [86]. The presence of organic acids (humic acid) additionally accelerates bacterial growth. In general, it is possible to significantly influence the antimicrobial activity of IONPs by additives, coatings, and conjugates, which, undoubtedly, can be promising in the development of this direction.

2.7. Biocompatibility of IONPs

It is shown that IONPs have good biocompatibility and biodegradability. In particular, the intravenous injection of 0.8 mg/kg of γ-Fe₂O₃ NPs did not influence the weight gain in rats or cause the activation of apoptosis in HUVEC cells [61]. After intravenous injection, NPs were found in rat lungs, liver, and kidneys but not in the brain or heart. A significant proportion of NPs was eliminated with urine after 72 h [61]. In general, IONPs show an absence or low cytotoxic effects on cell cultures. For example, no adverse effect of IONPs coated with polyethyleneimine, dimercaptosuccinate, or citrate on primary rat cerebellar cortex astrocytes and cultured murine astrocytes was observed [62,135]. IONPs conjugated with PEG-phospholipids (WFION) did not influence the viability of the B16 F10 cell line at doses up to 0.75-mg Fe/mL [136]. Fe₃O₄ NPs show a bacteriostatic effect and, at the same time, do not exert a hemolytic action [66,70]. In several cases, IONPs enhance Casp3-dependent apoptosis in HUVEC cells, cause ROS generation, membrane damage, changes in the cytoskeleton, and so on [137]. In general, the cytotoxic properties of IONPs are manifested at much higher concentrations than the antimicrobial properties.

2.8. Disadvantages of IONPs

The disadvantages of IONPs include relatively weak antimicrobial action against several strains and insufficient biocompatibility with eukaryotic cells. For example, Fe₂O₃ NPs inhibit the growth of *Escherichia coli*, *Staphylococcus aureus*, *Pseudomonas aeruginosa*, and *Bacillus subtilis* less effectively than ZnO and CuO NPs. The inhibitory action of Fe₂O₃ NPs on *Escherichia coli* growth was lower than that of ZnO and CuO NPs [138]. This effect may be explained by differences in the antibacterial properties of considered metals. Iron Fe²⁺ is necessary for the proliferation of bacteria [31]. Fe³⁺ inhibited *E. coli* growth in concentrations above 0.25–1 mM, but Fe³⁺ had only a bacteriostatic effect without bactericidal action [139]. Zn²⁺ and Cu⁺ decrease the viability of *Staphylococcus aureus* and *Escherichia coli* in concentrations of 2.41 and 0.46 mM, respectively [140]. Fe NPs exert more pronounced bacteriostatic actions against *Pseudomonas aeruginosa* than Fe₃O₄ NPs [84]. Lee et al. [97] did not observe the bactericidal action of Fe₃O₄ NPs against *E. coli* contrary to Fe NPs, Ag NPs, or FeSO₄ NPs. Fe²⁺ from IONPs in the presence of humic acid can enhance the growth of *Pseudomonas aeruginosa* [86]. The bacteriostatic action of Fe₃O₄ NPs against various microbial species differs significantly [8]. Fe₃O₄ NPs effectively inhibits the growth of *Staphylococcus epidermidis*, *Staphylococcus aureus*, *Bacillus licheniformis*, and *Bacillus subtilis*. The effect is comparable with the action of neomycin. With that, Fe₃O₄ NPs are two times less effective at inhibiting the growth of *Bacillus brevis* and *Vibrio cholerae* than neomycin and absolutely do not influence the growth of *Shigella flexneri* and *Pseudomonas aeruginosa*.

Unfortunately, IONPs has not only bacteriostatic and bactericidal activities but toxicity for some eukaryotic cell lines [108]. The main mechanism of IONP toxicity is the production of ROS, which leads to increasing the level of lipid peroxidation, decreasing the antioxidant enzymes, and protein aggregation [141–144]. IONPs can lead to cell iron overload. Iron overload causes serious deleterious and leads to cell death [142,143]. In addition, a high dose of IONPs increases the lipid metabolism, the breakage of iron homeostasis, and exacerbates the loss of murine liver functions in vivo [145].

The IONP applications in biomedicine are limited due to a lack of control and prediction of the final IONP properties, such as IONP interactions with cells [146]. An important aspect of IONPs in biomedical applications is their surface chemistry [147]. The coating of IONPs by PEG reduces protein adsorption, increases stability to the IONPs, decreases the IONP uptake by culture cells in and by entire organisms in vivo, and increases IONP retention times in the blood flow [148–150]. Unfortunately, PEG can be oxidized by host enzymes, which leads to a loss of some PEG-IONP proteins [148]. Proteins are commonly the first biomolecules that IONPs encounter when they interact with biological systems in vitro or in vivo [146]. IONPs may be coated by bovine serum albumin (BSA) or fetal bovine serum [151]. BSA forms a protective layer on the NPs to improve the biocompatibility and transport of the IONPs. BSA-coated IONPs allow to accumulate the drug in the tumor due to an enhanced permeability and retention and to reduce the risk of hypersensitivity reactions [152]. Drugs released from BSA-coated IONPs can be triggered by protease digestion in target tissues, and finally, the unfolding BSA protein on the IONPs can facilitate their clearance by phagocytes after drug delivery [153]. Additionally, BSA coating supports the colloidal stability of the IONPs in cell culture experiments [151]. Multiple specialized characterization methods are widely used to characterize IONP surfaces: TEM, UV-visualization, MD simulation, isothermal titration calorimetry, ζ-potential measuring, etc. [151]. The antibacterial properties of BSA-IONPs remain unclear.

3. Conclusions

IONPs have found wide applications in different fields of biomedicine. The antibacterial activities of IONPs are of special interest. However, the situation with the antimicrobial activities of IONPs is ambiguous. On the one hand, the antibacterial activities of IONPs depend, to a significant extent, on the microbial strain, and the inhibitory actions of IONPs are often less pronounced than that of NPs of other metal oxides (CuO or ZnO). On the other hand, IONPs show less-pronounced cytotoxic properties and better biocompatibility

in vivo compared to CuO or ZnO NPs. We assume that, in the near future, IONPs will allow achieving a balance between antimicrobial actions and biocompatibility in vivo. In this case, IONPs can be considered potential antimicrobial agents of the new generation. Based on the analyzed data, we believe that the most promising method for increasing the antimicrobial properties of IONPs and improving biocompatibility is “green synthesis” and other variants of the additive or composite generation of nanoparticles.

Author Contributions: Conceptualization, S.V.G.; writing—original draft preparation, D.E.B., D.A.S., M.B.R., and S.V.G.; visualization, D.A.S.; supervision, A.A.S.; and project administration, A.B.L. All authors have read and agreed to the published version of the manuscript.

Funding: This research was funded by the Ministry of Science and Education of the Russian Federation, grant number 075-15-2020-775.

Institutional Review Board Statement: Not applicable.

Informed Consent Statement: Not applicable.

Data Availability Statement: The raw data supporting the conclusions of this article will be made available by the authors without undue reservation.

Conflicts of Interest: The authors declare no conflict of interest.

References

- Wang, E.C.; Wang, A.Z. Nanoparticles and their applications in cell and molecular biology. *Integr. Biol.* **2014**, *6*, 9–26. [\[CrossRef\]](#)
- Thakur, N.; Manna, P.; Das, J. Synthesis and biomedical applications of nanoceria, a redox active nanoparticle. *J. Nanobiotechnol.* **2019**, *17*, 84. [\[CrossRef\]](#) [\[PubMed\]](#)
- Rajakumar, G.; Mao, L.; Bao, T.; Wen, W.; Wang, S.; Gomathi, T.; Gnanasundaram, N.; Rebezov, M.; Shariati, M.A.; Chung, I.-M.; et al. Yttrium Oxide Nanoparticle Synthesis: An Overview of Methods of Preparation and Biomedical Applications. *Appl. Sci.* **2021**, *11*, 2172. [\[CrossRef\]](#)
- Ahmad, B.; Shireen, F.; Rauf, A.; Shariati, M.A.; Bashir, S.; Patel, S.; Khan, A.; Rebezov, M.; Khan, M.U.; Mubarak, M.S.; et al. Phyto-fabrication, purification, characterisation, optimisation, and biological competence of nano-silver. *IET Nanobiotechnol.* **2021**, *15*, 1–18. [\[CrossRef\]](#)
- AlMatar, M.; Makky, E.A.; Var, I.; Koksai, F. The role of nanoparticles in the inhibition of multidrug-resistant bacteria and biofilms. *Curr. Drug Deliv.* **2018**, *15*, 470–484. [\[CrossRef\]](#)
- Su, Y.; Wu, D.; Xia, H.; Zhang, C.; Shi, J.; Wilkinson, K.J.; Xie, B. Metallic nanoparticles induced antibiotic resistance genes attenuation of leachate culturable microbiota: The combined roles of growth inhibition, ion dissolution and oxidative stress. *Environ. Int.* **2019**, *128*, 407–416. [\[CrossRef\]](#) [\[PubMed\]](#)
- Kim, J.S.; Kuk, E.; Yu, K.N.; Kim, J.H.; Park, S.J.; Lee, H.J.; Kim, S.H.; Park, Y.K.; Park, Y.H.; Hwang, C.Y.; et al. Antimicrobial effects of silver nanoparticles. *Nanomedicine* **2007**, *3*, 95–101. [\[CrossRef\]](#)
- Saliani, M.; Jalal, R.; Goharshadi, K.E. Effects of pH and temperature on antibacterial activity of zinc oxide nanofluid against *Escherichia coli* O157: H7 and *Staphylococcus aureus*. *Jundishapur J. Microbiol.* **2015**, *8*, e17115. [\[CrossRef\]](#)
- Behera, S.S.; Patra, J.K.; Pramanik, K.; Panda, N.; Thatoi, H. Characterization and evaluation of antibacterial activities of chemically synthesized iron oxide nanoparticles. *World J. Nano Sci. Eng.* **2012**, *2*, 196–200. [\[CrossRef\]](#)
- Allahverdiyev, A.M.; Abamor, E.S.; Bagirova, M.; Rafailovich, M. Antimicrobial effects of TiO₂ and Ag₂O nanoparticles against drug-resistant bacteria and leishmania parasites. *Future Microbiol.* **2011**, *6*, 933–940. [\[CrossRef\]](#) [\[PubMed\]](#)
- Khan, M.F.; Ansari, A.H.; Hameedullah, M.; Ahmad, E.; Husain, F.M.; Zia, Q.; Baig, U.; Zaheer, M.R.; Alam, M.M.; Khan, A.M.; et al. Sol-gel synthesis of thorn-like ZnO nanoparticles endorsing mechanical stirring effect and their antimicrobial activities: Potential role as nano-antibiotics. *Sci. Rep.* **2016**, *6*, 27689. [\[CrossRef\]](#)
- Ren, G.; Hu, D.; Cheng, E.W.C.; Vargas-Reus, M.A.; Reip, P.; Allaker, R.P. Characterisation of copper oxide nanoparticles for antimicrobial applications. *Int. J. Antimicrob. Agents* **2009**, *33*, 587–590. [\[CrossRef\]](#) [\[PubMed\]](#)
- Ahmed, T.; Wu, Z.; Jiang, H.; Luo, J.; Noman, M.; Shahid, M.; Manzoor, I.; Allemailem, K.S.; Alrumaihi, F.; Li, B. Bioinspired Green Synthesis of Zinc Oxide Nanoparticles from a Native *Bacillus cereus* Strain RNT6: Characterization and Antibacterial Activity against Rice Panicle Blight Pathogens *Burkholderia glumae* and *B. gladioli*. *Nanomaterials* **2021**, *11*, 884. [\[CrossRef\]](#)
- Gudkov, S.V.; Burmistrov, D.E.; Serov, D.A.; Rebezov, M.E.; Semenova, A.A.; Lisitsyn, A.B. A mini review of antibacterial properties of ZnO nanoparticles. *Front. Phys.* **2021**, *9*, 641481. [\[CrossRef\]](#)
- Pushcharovsky, D.Y. Iron and its compounds in the Earth's core: New data and ideas. *Geochem. Int.* **2019**, *57*, 941–955. [\[CrossRef\]](#)
- Pilchin, A.; Eppelbaum, L.V. *Iron and Its Unique Role in Earth Evolution*, 1st ed.; Geoph. Society: Mexico City, Mexico, 2006; ISBN 970-32-4122-0.
- Beinert, H.; Holm, R.H.; Munck, E. Iron-sulfur clusters: Nature's modular, multipurpose structures. *Science* **1997**, *277*, 653–659. [\[CrossRef\]](#)

18. Andreini, C.; Bertini, I.; Cavallaro, G.; Holliday, G.L.; Thornton, J.M. Metal ions in biological catalysis: From enzyme databases to general principles. *J. Biol. Inorg. Chem.* **2008**, *13*, 1205–1218. [[CrossRef](#)]
19. Caza, M.; Kronstad, J.W. Shared and distinct mechanisms of iron acquisition by bacterial and fungal pathogens of humans. *Front. Cell. Infect. Microbiol.* **2013**, *3*, 80. [[CrossRef](#)]
20. Andrews, S.C.; Robinson, A.K.; Rodriguez-Quinones, F. Bacterial iron homeostasis. *FEMS Microbiol. Rev.* **2003**, *27*, 215–237. [[CrossRef](#)]
21. Bagg, A.; Neilands, J.B. Ferric uptake regulation protein acts as a repressor, employing iron (II) as a cofactor to bind the operator of an iron transport operon in *Escherichia coli*. *Biochemistry* **1987**, *26*, 5471–5477. [[CrossRef](#)] [[PubMed](#)]
22. Fink, R.C.; Evans, M.R.; Porwollik, S.; Vazquez-Torres, A.; Jones-Carson, J.; Troxell, B.; Libby, S.J.; McClelland, M.; Hassan, H.M. FNR is a global regulator of virulence and anaerobic metabolism in *Salmonella enterica* serovar Typhimurium (ATCC 14028 s). *J. Bacteriol.* **2007**, *189*, 2262–2273. [[CrossRef](#)] [[PubMed](#)]
23. D’Autreaux, B.; Tucker, N.P.; Dixon, R.; Spiro, S. A non-haem iron centre in the transcription factor NorR senses nitric oxide. *Nature* **2005**, *437*, 769–772. [[CrossRef](#)] [[PubMed](#)]
24. Pomposiello, P.J.; Demple, B. Identification of SoxS-regulated genes in *Salmonella enterica* serovar typhimurium. *J. Bacteriol.* **2000**, *182*, 23–29. [[CrossRef](#)] [[PubMed](#)]
25. Schwartz, C.J.; Giel, J.L.; Patschkowski, T.; Luther, C.; Ruzicka, F.J.; Beinert, H.; Kiley, P.J. IscR, an Fe-S cluster-containing transcription factor, represses expression of *Escherichia coli* genes encoding Fe-S cluster assembly proteins. *Proc. Natl. Acad. Sci. USA* **2001**, *98*, 14895–14900. [[CrossRef](#)] [[PubMed](#)]
26. Karlinsey, J.E.; Bang, I.S.; Becker, L.A.; Frawley, E.R.; Porwollik, S.; Robbins, H.F.; Thomas, V.C.; Urbano, R.; McClelland, M.; Fang, F.C. The NsrR regulon in nitrosative stress resistance of *Salmonella enterica* serovar Typhimurium. *Mol. Microbiol.* **2012**, *85*, 1179–1193. [[CrossRef](#)]
27. Amor, M.; Ceballos, A.; Wan, J.; Simon, C.P.; Aron, A.T.; Chang, C.J.; Hellman, F.; Komeili, A. Magnetotactic Bacteria Accumulate a Large Pool of Iron Distinct from Their Magnetite Crystals. *Appl. Environ. Microbiol.* **2020**, *86*, e01278–20. [[CrossRef](#)]
28. Uebe, R.; Schüler, D. Magnetosome biogenesis in magnetotactic bacteria. *Nat. Rev. Microbiol.* **2016**, *14*, 621–637. [[CrossRef](#)]
29. Smith, M.J.; Sheehan, P.E.; Perry, L.L.; O’Connor, K.; Csonka, L.N.; Applegate, B.M.; Whitman, L.J. Quantifying the magnetic advantage in magnetotaxis. *Biophys. J.* **2006**, *91*, 1098–1107. [[CrossRef](#)]
30. Emerson, D.; Fleming, E.J.; McBeth, J.M. Iron-oxidizing bacteria: An environmental and genomic perspective. *Annu. Rev. Microbiol.* **2010**, *64*, 561–583. [[CrossRef](#)]
31. Parrow, N.L.; Fleming, R.E.; Minnick, M.F. Sequestration and scavenging of iron in infection. *Infect. Immun.* **2013**, *81*, 3503–3514. [[CrossRef](#)]
32. Tran, N.; Mir, A.; Mallik, D.; Sinha, A.; Nayar, S.; Webster, T.J. Bactericidal effect of iron oxide nanoparticles on *Staphylococcus aureus*. *Int. J. Nanomed.* **2010**, *5*, 277–283. [[CrossRef](#)]
33. Saqib, S.; Munis, M.F.H.; Zaman, W.; Ullah, F.; Shah, S.N.; Ayaz, A.; Farooq, M.; Bahadur, S. Synthesis, characterization and use of iron oxide nano particles for antibacterial activity. *Microsc. Res. Tech.* **2019**, *82*, 415–420. [[CrossRef](#)] [[PubMed](#)]
34. Fenton, H.J.H. Oxidation of tartaric acid in presence of iron. *J. Chem. Soc.* **1894**, *65*, 899–911. [[CrossRef](#)]
35. Frawley, E.R.; Fang, F.C. The ins and outs of bacterial iron metabolism. *Mol. Microbiol.* **2014**, *93*, 609–616. [[CrossRef](#)]
36. Sihem, L.; Hanine, D.; Faiza, B. Antibacterial Activity of α -Fe₂O₃ and α -Fe₂O₃@ Ag Nanoparticles Prepared by *Urtica* Leaf Extract. *Nanotechnol. Russ.* **2020**, *15*, 198–203. [[CrossRef](#)]
37. Li, D.; Shen, M.; Xia, J.; Shi, X. Recent developments of cancer nanomedicines based on ultrasmall iron oxide nanoparticles and nanoclusters. *Nanomedicine* **2021**, *16*, 609–612. [[CrossRef](#)]
38. Baimler, I.V.; Lisitsyn, A.B.; Serov, D.A.; Astashev, M.E.; Gudkov, S.V. Analysis of acoustic signals during the optical breakdown of aqueous solutions of Fe nanoparticles. *Front. Phys.* **2020**, *8*, 622551. [[CrossRef](#)]
39. Gudkov, S.V.; Baimler, I.V.; Uvarov, O.V.; Smirnova, V.V.; Volkov, M.Y.; Semenova, A.A.; Lisitsyn, A.B. Influence of the concentration of Fe and Cu nanoparticles on the dynamics of the size distribution of nanoparticles. *Front. Phys.* **2020**, *8*, 622551. [[CrossRef](#)]
40. Baimler, I.V.; Lisitsyn, A.B.; Gudkov, S.V. Water decomposition occurring during laser breakdown of aqueous solutions containing individual gold, zirconium, molybdenum, iron or nickel nanoparticles. *Front. Phys.* **2020**, *8*, 620938. [[CrossRef](#)]
41. Stolyar, S.V.; Krasitskaya, V.V.; Frank, L.A.; Yaroslavtsev, R.N.; Chekanova, L.A.; Gerasimova, Y.V.; Volochaev, M.N.; Bairmani, M.S.; Velikanov, D.A. Polysaccharide-coated iron oxide nanoparticles: Synthesis, properties, surface modification. *Mater. Lett.* **2021**, *284*, 128920. [[CrossRef](#)]
42. Tyurikova, I.A.; Alexandrov, S.E.; Tyurikov, K.S.; Kirilenko, D.A.; Speshilova, A.B.; Shakhmin, A.L. Fast and controllable synthesis of core-shell Fe₃O₄-C nanoparticles by aerosol CVD. *ACS Omega* **2020**, *5*, 8146–8150. [[CrossRef](#)]
43. Lozhkomoev, A.S.; Pervikov, A.V.; Kazantsev, S.O.; Sharipova, A.F.; Rodkevich, N.G.; Toropkov, N.E.; Suliz, K.V.; Svarovskaya, N.V.; Kondranova, A.M.; Lerner, M.I. Synthesis of Fe/Fe₃O₄ core-shell nanoparticles by electrical explosion of the iron wire in an oxygen-containing atmosphere. *J. Nanopart. Res.* **2021**, *23*, 73. [[CrossRef](#)]
44. Xie, J.; Chen, K.; Huang, J.; Lee, S.; Wang, J.; Gao, J.; Li, X.; Chen, X. PET/NIRF/MRI triple functional iron oxide nanoparticles. *Biomaterials* **2010**, *31*, 3016–3022. [[CrossRef](#)]
45. Emily, A. Waters SAW Contrast agents for MRI. *Basic Res. Cardiol.* **2008**, *103*, 114–121. [[CrossRef](#)]

46. Liu, J.; Xu, J.; Zhou, J.; Zhang, Y.; Guo, D.; Wang, Z. Fe₃O₄-based PLGA nanoparticles as MR contrast agents for the detection of thrombosis. *Int. J. Nanomed.* **2017**, *12*, 1113–1126. [[CrossRef](#)]
47. Cormode, D.P.; Naha, P.C.; Fayad, Z.A. Nanoparticle contrast agents for computed tomography: A focus on micelles. *Contrast Media Mol. Imaging* **2014**, *9*, 37–52. [[CrossRef](#)] [[PubMed](#)]
48. Thomas, R.; Park, I.K.; Jeong, Y.Y. Magnetic iron oxide nanoparticles for multimodal imaging and therapy of cancer. *Int. J. Mol. Sci.* **2013**, *14*, 15910–15930. [[CrossRef](#)]
49. Torres Martin de Rosales, R.; Tavaré, R.; Paul, R.L.; Jauregui-Osoro, M.; Protti, A.; Glaria, A.; Varma, G.; Szanda, I.; Blower, P.J. Synthesis of 64 Cu(II)-bis(dithiocarbamatebisphosphonate) and its conjugation with superparamagnetic iron oxide nanoparticles: In vivo evaluation as dual-modality PET-MRI agent. *Angew. Chem. Int. Ed. Engl.* **2011**, *50*, 5509–5513. [[CrossRef](#)]
50. Espinosa, A.; Di Coratom, R.; Kolosnjaj-Tabi, J.; Flaud, P.; Pellegrino, T.; Wilhelm, C. Duality of iron oxide nanoparticles in cancer therapy: Amplification of heating efficiency by magnetic hyperthermia and photothermal bimodal treatment. *ACS Nano* **2016**, *10*, 2436–2446. [[CrossRef](#)]
51. Vilas-Boas, V.; Espiña, B.; Kolen'ko, Y.V.; Bañobre-López, M.; Brito, M.; Martins, V.; Duarte, J.A.; Petrovykh, D.Y.; Freitas, P.; Carvalho, F. Effectiveness and safety of a nontargeted boost for a CXCR4-targeted magnetic hyperthermia treatment of cancer cells. *ACS Omega* **2019**, *4*, 1931–1940. [[CrossRef](#)]
52. Vilas-Boas, V.; Carvalho, F.; Espiña, B. Magnetic hyperthermia for cancer treatment: Main parameters affecting the outcome of in vitro and in vivo studies. *Molecules* **2020**, *25*, 2874. [[CrossRef](#)]
53. Shen, S.; Kong, F.; Guo, X.; Wu, L.; Shen, H.; Xie, M.; Wang, X.; Jin, Y.; Ge, Y. CMCTS stabilized Fe₃O₄ particles with extremely low toxicity as highly efficient near-infrared photothermal agents for in vivo tumor ablation. *Nanoscale* **2013**, *5*, 8056–8066. [[CrossRef](#)]
54. Tamanaha, C.R.; Mulvaney, S.P.; Rife, J.C.; Whitman, L.J. Magnetic labeling, detection, and system integration. *Biosens. Bioelectron.* **2008**, *24*, 1–13. [[CrossRef](#)]
55. Freitas, P.P.; Cardoso, F.A.; Martins, V.C.; Martins, S.A.; Loureiro, J.; Amaral, J.; Chaves, R.C.; Cardoso, S.; Fonseca, L.P.; Sebastião, A.M.; et al. Spintronic platforms for biomedical applications. *Lab Chip* **2012**, *12*, 546–557. [[CrossRef](#)]
56. Kaushik, A.; Khan, R.; Solanki, P.R.; Pandey, P.; Alam, J.; Ahmad, S.; Malhotra, B. Iron oxide nanoparticles–chitosan composite based glucose biosensor. *Biosens. Bioelectron.* **2008**, *24*, 676–683. [[CrossRef](#)]
57. Guldris, N.; Argibay, B.; Gallo, J.; Iglesias-Rey, R.; Carbó-Argibay, E.; Kolen'ko, Y.V.; Campos, F.; Sobrino, T.; Salonen, L.M.; Bañobre-López, M.; et al. Magnetite nanoparticles for stem cell labeling with high efficiency and long-term in vivo tracking. *Bioconjug. Chem.* **2017**, *28*, 362–370. [[CrossRef](#)]
58. Arachchige, M.P.; Laha, S.S.; Naik, A.R.; Lewis, K.T.; Naik, R.; Jena, B.P. Functionalized nanoparticles enable tracking the rapid entry and release of doxorubicin in human pancreatic cancer cells. *Micron* **2017**, *92*, 25–31. [[CrossRef](#)]
59. Borroni, E.; Miola, M.; Ferraris, S.; Ricci, G.; Zuzek Rozman, K.; Kostevsek, N.; Catizone, A.; Rimondini, L.; Prat, M.; Verne, E.; et al. Tumor targeting by lentiviral vectors combined with magnetic nanoparticles in mice. *Acta Biomater.* **2017**, *59*, 303–316. [[CrossRef](#)]
60. Markides, H.; Rotherham, M.; El Haj, A.J. Biocompatibility and toxicity of magnetic nanoparticles in regenerative medicine. *J. Nanomater.* **2012**, *13*. [[CrossRef](#)]
61. Hanini, A.; Schmitt, A.; Kacem, K.; Chau, F.; Ammar, S.; Gavard, J. Evaluation of iron oxide nanoparticle biocompatibility. *Int. J. Nanomed.* **2011**, *6*, 787–794. [[CrossRef](#)]
62. Yiu, H.H.; Pickard, M.R.; Olariu, C.I.; Williams, S.R.; Chari, D.M.; Rosseinsky, M.J. Fe₃O₄-PEI-RITC magnetic nanoparticles with imaging and gene transfer capability: Development of a tool for neural cell transplantation therapies. *Pharm. Res.* **2012**, *29*, 1328–1343. [[CrossRef](#)]
63. Gong, Y.; Ji, Y.; Liu, F.; Li, J.; Cao, Y. Cytotoxicity, oxidative stress and inflammation induced by ZnO nanoparticles in endothelial cells: Interaction with palmitate or lipopolysaccharide. *J. Appl. Toxicol.* **2017**, *37*, 895–901. [[CrossRef](#)] [[PubMed](#)]
64. Bai, X.; Li, L.; Liu, H.; Tan, L.; Liu, T.; Meng, X. Solvothermal synthesis of ZnO nanoparticles and anti-infection application in vivo. *ACS Appl. Mater. Interfaces* **2015**, *7*, 1308–1317. [[CrossRef](#)]
65. Kanoksil, M.; Jatapai, A.; Peacock, S.J.; Limmathurotsakul, D. Epidemiology, microbiology and mortality associated with community-acquired bacteremia in northeast Thailand: A multicenter surveillance study. *PLoS ONE* **2013**, *8*, e54714. [[CrossRef](#)]
66. Gabrielyan, L.; Hovhannisyan, A.; Gevorgyan, V.; Ananyan, M.; Trchounian, A. Antibacterial effects of iron oxide (Fe₃O₄) nanoparticles: Distinguishing concentration-dependent effects with different bacterial cells growth and membrane-associated mechanisms. *Appl. Microbiol. Biotechnol.* **2019**, *103*, 2773–2782. [[CrossRef](#)]
67. Janani, B.; Al-Mohaimed, A.M.; Raju, L.L.; Al Farraj, D.A.; Thomas, A.M.; Khan, S.S. Synthesis and characterizations of hybrid PEG-Fe₃O₄ nanoparticles for the efficient adsorptive removal of dye and antibacterial, and antibiofilm applications. *J. Environ. Health Sci. Eng.* **2021**, 1–12. [[CrossRef](#)]
68. Rufus, A.; Sreeju, N.; Philip, D. Synthesis of biogenic hematite (α-Fe₂O₃) nanoparticles for antibacterial and nanofluid applications. *RSC Adv.* **2016**, *6*, 94206–94217. [[CrossRef](#)]
69. Li, W.; Wei, W.; Wu, X.; Zhao, Y.; Dai, H. The antibacterial and antibiofilm activities of mesoporous hollow Fe₃O₄ nanoparticles in an alternating magnetic field. *Biomater. Sci.* **2020**, *8*, 4492–4507. [[CrossRef](#)]
70. Irshad, R.; Tahir, K.; Li, B.; Ahmad, A.; Siddiqui, A.R.; Nazir, S. Antibacterial activity of biochemically capped iron oxide nanoparticles: A view towards green chemistry. *J. Photochem. Photobiol. B* **2017**, *170*, 241–246. [[CrossRef](#)]

71. Al-Shabib, N.A.; Husain, F.M.; Ahmed, F.; Khan, R.A.; Khan, M.S.; Ansari, F.A.; Alam, M.Z.; Ahmed, M.A.; Khan, M.S.; Baig, M.H.; et al. Low temperature synthesis of superparamagnetic iron oxide (Fe₃O₄) nanoparticles and their ROS mediated inhibition of biofilm formed by food-associated bacteria. *Front. Microbiol.* **2018**, *9*, 2567. [[CrossRef](#)]
72. Fracasso, G.; Ghigna, P.; Nodari, L.; Agnoli, S.; Badocco, D.; Pastore, P.; Nicolato, E.; Marzola, P.; Mihajlović, D.; Markovic, M.; et al. Nanoaggregates of iron poly-oxo-clusters obtained by laser ablation in aqueous solution of phosphonates. *J. Colloid Interface Sci.* **2018**, *522*, 208–216. [[CrossRef](#)]
73. Arokiyaraj, S.; Saravanan, M.; Prakash, N.U.; Arasu, M.V.; Vijayakumar, B.; Vincent, S. Enhanced antibacterial activity of iron oxide magnetic nanoparticles treated with *Argemone mexicana* L. leaf extract: An in vitro study. *Mater. Res. Bull.* **2013**, *48*, 3323–3327. [[CrossRef](#)]
74. Vasantharaj, S.; Sathiyavimal, S.; Senthilkumar, P.; LewisOscar, F.; Pugazhendhi, A. Biosynthesis of iron oxide nanoparticles using leaf extract of *Ruellia tuberosa*: Antimicrobial properties and their applications in photocatalytic degradation. *J. Photochem. Photobiol. B* **2019**, *192*, 74–82. [[CrossRef](#)]
75. Chatterjee, S.; Bandyopadhyay, A.; Sarkar, K. Effect of iron oxide and gold nanoparticles on bacterial growth leading towards biological application. *J. Nanobiotechnol.* **2011**, *9*, 34. [[CrossRef](#)]
76. Bhushan, M.; Kumar, Y.; Periyasamy, L.; Viswanath, A.K. Antibacterial applications of α-Fe₂O₃/Co₃O₄ nanocomposites and study of their structural, optical, magnetic and cytotoxic characteristics. *Appl. Nanosci.* **2018**, *8*, 137–153. [[CrossRef](#)]
77. Khashan, K.S.; Sulaiman, G.M.; Mahdi, R. Preparation of iron oxide nanoparticles-decorated carbon nanotube using laser ablation in liquid and their antimicrobial activity. *Artif. Cells Nanomed. Biotechnol.* **2017**, *45*, 1699–1709. [[CrossRef](#)] [[PubMed](#)]
78. Arakha, M.; Pal, S.; Samantarrai, D.; Panigrahi, T.K.; Mallick, B.C.; Pramanik, K.; Mallick, B.; Jha, S. Antimicrobial activity of iron oxide nanoparticle upon modulation of nanoparticle-bacteria interface. *Sci. Rep.* **2015**, *5*, 14813. [[CrossRef](#)] [[PubMed](#)]
79. Bhattacharya, P.; Neogi, S. Gentamicin coated iron oxide nanoparticles as novel antibacterial agents. *Mater. Res. Express* **2017**, *4*, 095005. [[CrossRef](#)]
80. Amutha, S.; Sridhar, S. Green synthesis of magnetic iron oxide nanoparticle using leaves of *Glycosmis mauritiana* and their antibacterial activity against human pathogens. *J. Innov. Pharm. Biol. Sci.* **2015**, *29*, 22–26. [[CrossRef](#)]
81. Sathishkumar, G.; Logeshwaran, V.; Sarathbabu, S.; Jha, P.K.; Jeyaraj, M.; Rajkuberan, C.; Senthilkumar, N.; Sivaramakrishnan, S. Green synthesis of magnetic Fe₃O₄ nanoparticles using *Couroupita guianensis* Aubl. fruit extract for their antibacterial and cytotoxicity activities. *Artif. Cells Nanomed. Biotechnol.* **2018**, *46*, 589–598. [[CrossRef](#)]
82. Mousavi, S.M.; Hashemi, S.A.; Zarei, M.; Bahrani, S.; Savardashtaki, A.; Esmaili, H.; Lai, C.W.; Mazraedoost, S.; Abassi, M.; Ramavandi, B. Data on cytotoxic and antibacterial activity of synthesized Fe₃O₄ nanoparticles using *Malva sylvestris*. *Data Brief* **2019**, *28*, 104929. [[CrossRef](#)]
83. Prabhu, Y.T.; Rao, K.V.; Kumari, B.S.; Kumar, V.S.S.; Pavani, T. Synthesis of Fe₃O₄ nanoparticles and its antibacterial application. *Int. Nano Lett.* **2015**, *5*, 85–92. [[CrossRef](#)]
84. Armijo, L.M.; Wawrzyniec, S.J.; Kopciuch, M.; Brandt, Y.I.; Rivera, A.C.; Withers, N.J.; Cook, N.C.; Huber, D.L.; Monson, T.C.; Smyth, H.D.C.; et al. Antibacterial activity of iron oxide, iron nitride, and tobramycin conjugated nanoparticles against *Pseudomonas aeruginosa* biofilms. *J. Nanobiotechnol.* **2020**, *18*, 35. [[CrossRef](#)] [[PubMed](#)]
85. Velusamy, P.; Chia-Hung, S.; Shritama, A.; Kumar, G.V.; Jeyanthi, V.; Pandian, K. Synthesis of oleic acid coated iron oxide nanoparticles and its role in anti-biofilm activity against clinical isolates of bacterial pathogens. *J. Taiwan Inst. Chem. Eng.* **2016**, *59*, 450–456. [[CrossRef](#)]
86. Current, K.M.; Dissanayake, N.M.; Obare, S.O. Effect of iron oxide nanoparticles and amoxicillin on bacterial growth in the presence of dissolved organic carbon. *Biomedicines* **2017**, *5*, 55. [[CrossRef](#)] [[PubMed](#)]
87. Patra, J.K.; Ali, M.S.; Oh, I.G.; Baek, K.H. Proteasome inhibitory, antioxidant, and synergistic antibacterial and anticandidal activity of green biosynthesized magnetic Fe₃O₄ nanoparticles using the aqueous extract of corn (*Zea mays* L.) ear leaves. *Artif. Cells Nanomed. Biotechnol.* **2017**, *45*, 349–356. [[CrossRef](#)]
88. Groiss, S.; Selvaraj, R.; Varadavenkatesan, T.; Vinayagam, R. Structural characterization, antibacterial and catalytic effect of iron oxide nanoparticles synthesised using the leaf extract of *Cynometra ramiflora*. *J. Mol. Struct.* **2017**, *1128*, 572–578. [[CrossRef](#)]
89. Javanbakht, T.; Laurent, S.; Stanicki, D.; Wilkinson, K.J. Relating the surface properties of superparamagnetic iron oxide nanoparticles (SPIONs) to their bactericidal effect towards a biofilm of *Streptococcus mutans*. *PLoS ONE* **2016**, *11*, e0154445. [[CrossRef](#)]
90. Nehra, P.; Chauhan, R.P.; Garg, N.; Verma, K. Antibacterial and antifungal activity of chitosan coated iron oxide nanoparticles. *Br. J. Biomed. Sci.* **2018**, *75*, 13–18. [[CrossRef](#)]
91. Ismail, R.A.; Sulaiman, G.M.; Abdulrahman, S.A.; Marzoog, T.R. Antibacterial activity of magnetic iron oxide nanoparticles synthesized by laser ablation in liquid. *Mater. Sci. Eng. C Mater. Biol. Appl.* **2015**, *53*, 286–297. [[CrossRef](#)]
92. Bezza, F.A.; Tichapondwa, S.M.; Chirwa, E.M.N. Fabrication of monodispersed copper oxide nanoparticles with potential application as antimicrobial agents. *Sci. Rep.* **2020**, *10*, 16680. [[CrossRef](#)] [[PubMed](#)]
93. Yusof, N.A.A.; Zain, N.M.; Pauzi, N. Synthesis of ZnO nanoparticles with chitosan as stabilizing agent and their antibacterial properties against Gram-positive and Gram-negative bacteria. *Int. J. Biol. Macromol.* **2019**, *124*, 1132–1136. [[CrossRef](#)]
94. Kohanski, M.A.; DePristo, M.A.; Collins, J.J. Sublethal antibiotic treatment leads to multidrug resistance via radical-induced mutagenesis. *Mol. Cell* **2010**, *37*, 311–320. [[CrossRef](#)] [[PubMed](#)]

95. Yu, J.; Zhang, W.; Li, Y.; Wang, G.; Yang, L.; Jin, J.; Huang, M. Synthesis, characterization, antimicrobial activity and mechanism of a novel hydroxyapatite whisker/nano zinc oxide biomaterial. *Biomed. Mater.* **2014**, *10*, 015001. [[CrossRef](#)]
96. Sousa, C.; Sequeira, D.; Kolen'ko, Y.V.; Pinto, I.M.; Petrovykh, D.Y. Analytical protocols for separation and electron microscopy of nanoparticles interacting with bacterial cells. *Anal. Chem.* **2015**, *87*, 4641–4648. [[CrossRef](#)]
97. Lee, C.; Kim, J.Y.; Lee, W.I.; Nelson, K.L.; David, L.; Sedlak, D.L. Bactericidal effect of zero-valent iron nanoparticles on *Escherichia coli*. *Environ. Sci. Technol.* **2008**, *42*, 4927–4933. [[CrossRef](#)]
98. Guittat, L.; Alberti, P.; Rosu, F.; Van Miert, S.; Thetiot, E.; Pieters, L.; Gabelica, V.; De Pauw, E.; Ottaviani, A.; Riou, J.F.; et al. Interactions of cryptolepine and neocryptolepine with unusual DNA structures. *Biochimie* **2003**, *85*, 535–547. [[CrossRef](#)]
99. Li, Y.; Yang, D.; Wang, S.; Li, C.; Xue, B.; Yang, L.; Shen, Z.; Jin, M.; Wang, J.; Qiu, Z. The detailed bactericidal process of ferric oxide nanoparticles on *E. coli*. *Molecules* **2018**, *23*, 606. [[CrossRef](#)]
100. Morones, J.R.; Elechiguerra, J.L.; Camacho, A.; Holt, K.; Kouri, J.B.; Ramírez, J.T.; Yacaman, M.J. The bactericidal effect of silver nanoparticles. *Nanotechnology* **2005**, *16*, 2346–2353. [[CrossRef](#)] [[PubMed](#)]
101. Nel, A.E.; Mädler, L.; Velegol, D.; Xia, T.; Hoek, E.M.; Somasundaran, P.; Klaessig, F.; Castranova, V.; Thompson, M. Understanding biophysicochemical interactions at the nano-bio interface. *Nat. Mater.* **2009**, *8*, 543–557. [[CrossRef](#)] [[PubMed](#)]
102. Margabandhu, M.; Sendhilmathan, S.; Maragathavalli, S.; Karthikeyan, V.; Annadurai, B. Synthesis characterization and antibacterial activity of iron oxide nanoparticles. *Glob. J. Bio-Sci. Biotechnol.* **2015**, *4*, 335–341.
103. Kolen'ko, Y.V.; Bañobre-López, M.; Rodríguez-Abreu, C.; Carbó-Argibay, E.; Sailsman, A.; Piñeiro-Redondo, Y.; Cerqueira, M.F.; Petrovykh, D.Y.; Kovnir, K.; Lebed, O.A.; et al. Large-scale synthesis of colloidal Fe₃O₄ nanoparticles exhibiting high heating efficiency in magnetic hyperthermia. *J. Phys. Chem. C* **2014**, *118*, 8691–8701. [[CrossRef](#)]
104. Kolen'ko, Y.V.; Bañobre-López, M.; Rodríguez-Abreu, C.; Carbó-Argibay, E.; Deepak, F.L.; Petrovykh, D.Y.; Cerqueira, M.F.; Kamali, S.; Kovnir, K.; Shtansky, D.V.; et al. High-temperature magnetism as a probe for structural and compositional uniformity in ligand-capped magnetite nanoparticles. *J. Phys. Chem. C Nanomater. Interfaces* **2014**, *118*, 28322–28329. [[CrossRef](#)] [[PubMed](#)]
105. Ali, A.; Zafar, H.; Zia, M.; Ul Haq, I.; Phull, A.R.; Ali, J.S.; Hussain, A. Synthesis, characterization, applications, and challenges of iron oxide nanoparticles. *Nanotechnol. Sci. Appl.* **2016**, *9*, 49–67. [[CrossRef](#)] [[PubMed](#)]
106. Toropova, Y.G.; Zelinskaya, I.A.; Gorshkova, M.N.; Motorina, D.S.; Korolev, D.V.; Velikonitsev, F.S.; Gareev, K.G. Albumin covering maintains endothelial function upon magnetic iron oxide nanoparticles intravenous injection in rats. *J. Biomed. Mater. Res. Part A* **2021**. [[CrossRef](#)] [[PubMed](#)]
107. Omelchenko, A.; Sobol, E.; Simakin, A.; Serkov, A.; Sukhov, I.; Shafeev, G. Biofunctional magnetic 'core-shell' nanoparticles generated by laser ablation of iron in liquid. *Laser Phys.* **2015**, *25*, 025607. [[CrossRef](#)]
108. Arias, L.S.; Pessan, J.P.; Vieira, A.P.M.; Lima, T.M.T.; Delbem, A.C.B.; Monteiro, D.R. Iron Oxide Nanoparticles for Biomedical Applications: A Perspective on Synthesis, Drugs, Antimicrobial Activity, and Toxicity. *Antibiotics* **2018**, *7*, 46. [[CrossRef](#)] [[PubMed](#)]
109. Wu, W.; Wu, Z.; Yu, T.; Jiang, C.; Kim, W.S. Recent progress on magnetic iron oxide nanoparticles: Synthesis, surface functional strategies and biomedical applications. *Sci. Technol. Adv. Mater.* **2015**, *16*, 023501. [[CrossRef](#)]
110. Kansara, K.; Patel, P.; Shukla, R.K.; Pandya, A.; Shanker, R.; Kumar, A.; Dhawan, A. Synthesis of biocompatible iron oxide nanoparticles as a drug delivery vehicle. *Int. J. Nanomed.* **2018**, *13*, 79–82. [[CrossRef](#)] [[PubMed](#)]
111. Huang, Y.; Mao, K.; Zhang, B.; Zhao, Y. Superparamagnetic iron oxide nanoparticles conjugated with folic acid for dual target-specific drug delivery and MRI in cancer theranostics. *Mater. Sci. Eng. C Mater. Biol. Appl.* **2017**, *70*, 763–771. [[CrossRef](#)]
112. Riaz, S.; Bashir, M.; Naseem, S. Iron oxide nanoparticles prepared by modified co-precipitation method. *IEEE Trans. Magn.* **2014**, *50*, 1–4. [[CrossRef](#)]
113. Maity, D.; Ding, J.; Xue, J.M. Synthesis of magnetite nanoparticles by thermal decomposition: Time, temperature, surfactant and solvent effects. *Funct. Mater. Lett.* **2008**, *1*, 189–193. [[CrossRef](#)]
114. Yu, W.W.; Falkner, J.C.; Yavuz, C.T.; Colvin, V.L. Synthesis of monodisperse iron oxide nanocrystals by thermal decomposition of iron carboxylate salts. *Chem. Commun.* **2004**, *10*, 2306–2307. [[CrossRef](#)]
115. Hatakeyama, M.; Kishi, H.; Kita, Y.; Imai, K.; Nishio, K.; Karasawa, S.; Masaike, Y.; Sakamoto, S.; Sandhu, A.; Tanimoto, A.; et al. A two-step ligand exchange reaction generates highly water-dispersed magnetic nanoparticles for biomedical applications. *J. Mater. Chem.* **2011**, *21*, 5959–5966. [[CrossRef](#)]
116. Pandey, S.; Mishra, S.B. Sol-gel derived organic-inorganic hybrid materials: Synthesis, characterizations and applications. *J. Sol-Gel Sci. Technol.* **2011**, *59*, 73–94. [[CrossRef](#)]
117. Xu, J.K.; Zhang, F.F.; Sun, J.J.; Sheng, J.; Wang, F.; Sun, M. Bio and nanomaterials based on Fe₃O₄. *Molecules* **2014**, *19*, 21506–21528. [[CrossRef](#)]
118. Amendola, V.; Meneghetti, M. What controls the composition and the structure of nanomaterials generated by laser ablation in liquid solution? *Phys. Chem. Chem. Phys.* **2013**, *15*, 3027–3046. [[CrossRef](#)]
119. Pallela, P.N.V.K.; Ummey, S.; Ruddaraju, L.K.; Gadi, S.; Cherukuri, C.S.; Barla, S.; Pammi, S.V.N. Antibacterial efficacy of green synthesized α-Fe₂O₃ nanoparticles using *Sida cordifolia* plant extract. *Heliyon* **2019**, *5*, e02765. [[CrossRef](#)]
120. Senthil, M.; Ramesh, C. Biogenic synthesis of Fe₃O₄ nanoparticles using *Tridax procumbens* leaf extract and its antibacterial activity on *Pseudomonas aeruginosa*. *Dig. J. Nanomater. Biostruct.* **2012**, *7*, 1655–1660.
121. Bashir, M.; Ali, S.; Farrukh, M.A. Green synthesis of Fe₂O₃ nanoparticles from orange peel extract and a study of its antibacterial activity. *J. Korean Phys. Soc.* **2020**, *76*, 848–854. [[CrossRef](#)]

122. Mahmoudi, M.; Sant, S.; Wang, B.; Laurent, S.; Sen, T. Superparamagnetic iron oxide nanoparticles (SPIONs): Development, surface modification and applications in chemotherapy. *Adv. Drug Deliv. Rev.* **2011**, *63*, 24–46. [[CrossRef](#)]
123. Lu, A.H.; Salabas, E.L.; Schüth, F. Magnetic nanoparticles: Synthesis, protection, functionalization, and application. *Angew. Chem. Int. Ed. Engl.* **2007**, *46*, 1222. [[CrossRef](#)]
124. Maji, S.K.; Mukherjee, N.; Mondal, A.; Adhikary, B. Synthesis, characterization and photocatalytic activity of α -Fe₂O₃ nanoparticles. *Polyhedron* **2012**, *33*, 145–149. [[CrossRef](#)]
125. Mohapatra, M.; Anand, S. Synthesis and applications of nano-structured iron oxides/hydroxides—a review. *Int. J. Eng. Sci. Technol.* **2010**, *2*, 127–146. [[CrossRef](#)]
126. Upadhyay, S.; Parekh, K.; Pandey, B. Influence of crystallite size on the magnetic properties of Fe₃O₄ nanoparticles. *J. Alloys Compd.* **2016**, *678*, 478–485. [[CrossRef](#)]
127. Gabrielyan, L.; Hakobyan, L.; Hovhannisyanyan, A.; Trchounian, A. Effects of iron oxide (Fe₃O₄) nanoparticles on *Escherichia coli* antibiotic-resistant strains. *J. Appl. Microbiol.* **2019**, *126*, 1108–1116. [[CrossRef](#)] [[PubMed](#)]
128. Awwad, A.M.; Salem, N.M. A green and facile approach for synthesis of magnetite nanoparticles. *Nanosci. Nanotechnol.* **2012**, *2*, 208–213. [[CrossRef](#)]
129. Soenen, S.J.; Himmelreich, U.; Nuytten, N.; De Cuyper, M. Cytotoxic effects of iron oxide nanoparticles and implications for safety in cell labelling. *Biomaterials* **2011**, *32*, 195–205. [[CrossRef](#)]
130. Naeimi, H.; Nazifi, Z.S.; Amininezhad, S.M. Preparation of Fe₃O₄ encapsulated-silica sulfonic acid nanoparticles and study of their in vitro antimicrobial activity. *J. Photochem. Photobiol. B* **2015**, *149*, 180–188. [[CrossRef](#)]
131. Gabrielyan, L.; Badalyan, H.; Gevorgyan, V.; Trchounian, A. Comparable antibacterial effects and action mechanisms of silver and iron oxide nanoparticles on *Escherichia coli* and *Salmonella typhimurium*. *Sci. Rep.* **2020**, *10*, 13145. [[CrossRef](#)] [[PubMed](#)]
132. Ansari, S.A.; Oves, M.; Star, R.; Khan, A.; Ahmad, S.A.; Jafri, M.A.; Zaidi, S.K.; Algahtani, M.H.; Star, R.; Khan, A.; et al. Antibacterial activity of iron oxide nanoparticles synthesized by co-precipitation technology against *Bacillus cereus* and *Klebsiella pneumoniae*. *Polish J. Chem. Technol.* **2017**, *19*, 110–115. [[CrossRef](#)]
133. Lee, C.; Jeon, H.; Kim, S.; Kim, E.; Kim, D.W.; Lim, S.T.; Jang, K.Y.; Jeong, Y.Y.; Nah, J.W.; Sohn, M. SPION-loaded chitosan–linoleic acid nanoparticles to target hepatocytes. *Int. J. Pharm.* **2009**, *371*, 163–169. [[CrossRef](#)]
134. Maurizi, L.; Papa, A.; Boudon, J.; Sudhakaran, S.; Pruvot, B.; Vandroux, D.; Chluba, J.; Lizard, G.; Millot, N. Toxicological risk assessment of emerging nanomaterials: Cytotoxicity, cellular uptake, effects on biogenesis and cell organelle activity, acute toxicity and biodistribution of oxide nanoparticles. In *Unraveling the Safety Profile of Nanoscale Particles and Materials*; IntechOpen IntechOpen Limited: London, UK, 2018. [[CrossRef](#)]
135. Geppert, M.; Hohnholt, M.C.; Thiel, K.; Nürnberger, S.; Grunwald, I.; Rezwani, K.; Dringen, R. Uptake of dimercaptosuccinate-coated magnetic iron oxide nanoparticles by cultured brain astrocytes. *Nanotechnology* **2011**, *22*, 145101. [[CrossRef](#)] [[PubMed](#)]
136. Lee, N.; Choi, Y.; Lee, Y.; Park, M.; Moon, W.K.; Choi, S.H.; Hyeon, T. Water-dispersible ferrimagnetic iron oxide nanocubes with extremely high r₂ relaxivity for highly sensitive in vivo MRI of tumors. *Nano Lett.* **2012**, *12*, 3127–3131. [[CrossRef](#)]
137. Valdíglesias, V.; Fernández-Bertólez, N.; Kiliç, G.; Costa, C.; Costa, S.; Fraga, S.; Bessa, M.J.; Pásaro, E.; Teixeira, J.P.; Laffon, B. Are iron oxide nanoparticles safe? Current knowledge and future perspectives. *J. Trace Elem. Med. Biol.* **2016**, *38*, 53–63. [[CrossRef](#)]
138. Azam, A.; Ahmed, A.S.; Oves, M.; Khan, M.S.; Habib, S.S.; Memic, A. Antimicrobial activity of metal oxide nanoparticles against Gram-positive and Gram-negative bacteria: A comparative study. *Int. J. Nanomed.* **2012**, *7*, 6003–6009. [[CrossRef](#)]
139. Braun, V. Surface signaling: Novel transcription initiation mechanism starting from the cell surface. *Arch. Microbiol.* **1997**, *167*, 325–331. [[CrossRef](#)] [[PubMed](#)]
140. Yasuyuki, M.; Kunihiro, K.; Kurissery, S.; Kanavillil, N.; Sato, Y.; Kikuchi, Y. Antibacterial properties of nine pure metals: A laboratory study using *Staphylococcus aureus* and *Escherichia coli*. *Biofouling. J. Bioadhes. Biofilm Res.* **2010**, *26*, 851–858. [[CrossRef](#)] [[PubMed](#)]
141. Apopa, P.L.; Qian, Y.; Shao, R.; Guo, N.L.; Schwegler-Berry, D.; Pacurari, M.; Porter, D.; Shi, X.; Vallyathan, V.; Castranova, V.; et al. Iron oxide nanoparticles induce human microvascular endothelial cell permeability through reactive oxygen species production and microtubule remodeling. *Part. Fibre Toxicol.* **2009**, *6*, 1. [[CrossRef](#)] [[PubMed](#)]
142. Singh, N.; Jenkins, G.J.; Asadi, R.; Doak, S.H. Potential toxicity of superparamagnetic iron oxide nanoparticles (SPION). *Nano Rev.* **2010**, *1*, 5358. [[CrossRef](#)]
143. Yarjanli, Z.; Ghaedi, K.; Esmaeili, A.; Rahgozar, S.; Zarrabi, A. Iron oxide nanoparticles may damage to the neural tissue through iron accumulation, oxidative stress, and protein aggregation. *BMC Neurosci.* **2017**, *18*, 51. [[CrossRef](#)]
144. Dwivedi, S.; Siddiqui, M.A.; Farshori, N.N.; Ahamed, M.; Musarrat, J.; Al-Khedhairi, A.A. Synthesis, characterization and toxicological evaluation of iron oxide nanoparticles in human lung alveolar epithelial cells. *Colloids Surf. B Biointerfaces* **2014**, *122*, 209–215. [[CrossRef](#)]
145. Wei, Y.; Zhao, M.; Yang, F.; Mao, Y.; Xie, H.; Zhou, Q. Iron overload by superparamagnetic iron oxide nanoparticles is a high risk factor in cirrhosis by a systems toxicology assessment. *Sci. Rep.* **2016**, *6*, 29110. [[CrossRef](#)]
146. Petros, R.A.; DeSimone, J.M. Strategies in the design of nanoparticles for therapeutic applications. *Nat. Rev. Drug Discov.* **2010**, *9*, 615–627. [[CrossRef](#)]
147. Grainger, D.W. Connecting drug delivery reality to smart materials design. *Int. J. Pharm.* **2013**, *454*, 521–524. [[CrossRef](#)]

148. Pelaz, B.; del Pino, P.; Maffre, P.; Hartmann, R.; Gallego, M.; Rivera-Fernández, S.; de la Fuente, J.M.; Nienhaus, G.U.; Parak, W.J. Surface Functionalization of Nanoparticles with Polyethylene Glycol: Effects on Protein Adsorption and Cellular Uptake. *ACS Nano* **2015**, *9*, 6996–7008. [[CrossRef](#)]
149. Zhang, Y.; Kohler, N.; Zhang, M. Surface modification of superparamagnetic magnetite nanoparticles and their intracellular uptake. *Biomaterials* **2002**, *23*, 1553–1561. [[CrossRef](#)]
150. Xie, J.; Xu, C.; Kohler, N.; Hou, Y.; Sun, S. Controlled PEGylation of monodisperse Fe₃O₄ nanoparticles for reduced non-specific uptake by macrophage cells. *Adv. Mater.* **2007**, *19*, 3163–3166. [[CrossRef](#)]
151. Yu, S.; Perálvarez-Marín, A.; Minelli, C.; Faraudo, J.; Roig, A.; Laromaine, A. Albumin-coated SPIONs: An experimental and theoretical evaluation of protein conformation, binding affinity and competition with serum proteins. *Nanoscale* **2016**, *8*, 14393–14405. [[CrossRef](#)]
152. Kalidasan, V.; Liu, X.L.; Herng, T.S.; Yang, Y.; Ding, J. Bovine Serum Albumin-Conjugated Ferrimagnetic Iron Oxide Nanoparticles to Enhance the Biocompatibility and Magnetic Hyperthermia Performance. *Nanomicro Lett.* **2016**, *8*, 80–93. [[CrossRef](#)] [[PubMed](#)]
153. Maffre, P.; Brandholt, S.; Nienhaus, K.; Shang, L.; Parak, W.J.; Nienhaus, G.U. Effects of surface functionalization on the adsorption of human serum albumin onto nanoparticles—A fluorescence correlation spectroscopy study. *Beilstein J. Nanotechnol.* **2014**, *5*, 2036–2047. [[CrossRef](#)] [[PubMed](#)]